Available online at www.sciencedirect.com
SCIENCE DIRECT®
ELSEVIER
Mechanism and Machine Theory 39 (2004) 555–581
Mechanism and Machine Theory
www.elsevier.com/locate/mechmt

A multi-fingered hand prosthesis

Jingzhou Yang [a,*], Esteban Peña Pitarch [b], Karim Abdel-Malek [a], Amos Patrick [a], Lars Lindkvist [c]

[a] Digital Humans Laboratory, Center for Computer-Aided Design, The University of Iowa, 116 Engineering Research Facility, Iowa City, IA 52242-1000, USA
[b] Departament Enginyeria Mecanica, Universitat Politecnica De Catalvnya (UPC), Av. Bases de Manresa, 61–73, 08240 Manresa, Spain
[c] Machine and Vehicle Design, Chalmers University of Technology, Sweden

Received 8 November 2003; received in revised form 29 December 2003; accepted 12 January 2004

Abstract

Design and analysis of a multi-fingered hand prosthesis is presented. The hand has multi-actuated fingers, four with two joints and the thumb with three joints. Each joint is designed using a novel flexible mechanism based on the loading of a compression spring in both transverse and axial directions and using cable-conduit systems. The rotational motion is transformed to tendon-like behavior, which enables the location of the actuators far from the arm (e.g., on a belt around the waist). The forward kinematics of the mechanism is presented. It is shown that the solution of the transverse deflection of each finger segment is obtained in a general form through a Haringx model followed by an element stiffness model. A prototype finger is experimentally tested, results verified, and the hand prosthesis is built. This new design, while presents a low cost alternative, enables the actuation and control of a multi-fingered hand with relatively high degrees of freedom.

Keywords: Prosthetic design; Kinematics of hand prosthesis; Biomechanics of hand; Multi-fingered hand

1. Introduction

The design of body-powered upper-limb prostheses in particular has experienced few, if any, major breakthroughs since the early 1960s (see a review by Fletcher [9]; an article by Godden [10]; a book by Klopsteg and Wilson [17]; and a review by Lunteren et al. [25]). Persons with

* Corresponding author. Tel.: +1-319-353-2249; fax: +1-319-384-0542.
E-mail address: jyang@engineering.uiowa.edu (J. Yang).

0094-114X/$ - see front matter
doi:10.1016/j.mechmachtheory.2004.01.002

amputation frequently express dissatisfaction with the current state of upper-limb prosthesis technology [8,11,13,14,20,21,27] noting numerous deficiencies with their prostheses. Yet continued advances in materials science will undoubtedly yield significantly improved functionality and far better esthetics.

Upper-limb prostheses are either hook or hand-shaped, and are actuated by body or external power. In the United States, approximately 70% of users wear hooks. Outside the United States, especially in developing countries, there is a greater preference for hand-shaped prostheses. Compared to hooks, prosthetic hands generally offer less function and durability at greater weight and cost. Nonetheless, many individuals still choose hands over hooks, primarily for cosmetic reasons [7].

The development of an upper-limb prosthesis that can be felt as a part of the body by the amputee is far to become reality. In fact, current commercial prosthesis hands are unable to provide enough grasping functionality. One of the main problems of the current available devices is the lack of the degrees of freedom (DOFs).

Some examples of research on multi-fingered hands can be found in the work of Hanafusa and Asadas [12], Okada [30] and Skinner [36]. The Okada hand was a three-fingered cable-driven hand which accomplished tasks such as attaching a nut to a bolt. Hanafusa and Asadas hand has three elastic fingers driven by a single motor with three claws for stably grasping several oddly shaped objects. Later multi-fingered hands include the Salisbury Hand (Stanford/JPL hand) [26], the Utah/MIT hand [15], the NYU hand [6] and the research hand Styx [28]. The Salisbury hand is a three-fingered hand; each finger has three degrees of freedom and the joints are all cable driven by electric motors. The placement of the fingers consist of one finger (the thumb) opposing the other two. The Utah/MIT hand has four fingers (three fingers and a thumb), in a very anthropomorphic configuration; each finger has four degrees of freedom and the hand is cable driven by pneumatic pistons. The NYU hand is a non-anthropomorphic planar hand with four fingers moving in a plane, driven by stepper motors. Styx was a two fingered hand with each finger having two joints, all direct driven. Like the NYU hand, Styx was used as a test bed for performing control experiments on multi-fingered hands.

Commercially available prosthesis devices, such as Otto Bock SeneorHand^{TM}, as well as multifunctional hand designs [1,2,4,7,21,35], are far from providing the manipulation capabilities of the human hand [5]. This is due to many different reasons. For example, in prosthetic hands active bending is restricted to two or three joints, which are actuated by a single motor drive acting simultaneously on the metacarpo-phalangeal (MCP) joints of the thumb, of the index and of the middle finger, while other joints can bend only passively.

Over the past 20 years the myoelectrically controlled hand prosthesis for children, first introduced by researchers from Sweden and the Netherlands [3,18,19,24,32,33] has become one of the standard prosthetic devices for children with a unilateral below elbow defect. This type of prosthesis is very well accepted because of its appearance and the absence of a control harness despite stated disadvantages: heavy, slow operating speed, vulnerable and its size prohibits fitting to children with a long forearm stump. Recent advances include specific factors related to voluntary pinching [13,14,34], underarticulation [22], multifunctionality of a hand [37] and forces at the fingertips [29]. Some active and passive prosthetic hands are shown in Fig. 1.

The aim of this paper is to introduce the IOWA hand, to illustrate the unique mechanism used to actuate each joint, and to present the analysis used in controlling the hand. In the recent

(a) (b) (c) (d)

Fig. 1. (a) Otto Bock electrohand. (b) Becker Imperial hand. (c) PMR modular electric. (d) APRL hand.

research [38] we developed one closed form solution, however, it is unstable in some cases and this paper presents a more efficient model (Haringx model) in two dimensional analysis and introduces another solution in three dimensional model (element stiffness model).

2. The IOWA hand

The IOWA hand prosthesis was designed and built at the University of Iowa using a novel approach to the design of multi-segmental joints with the objective to actuate each finger using a cable-conduit system. Each segment of a finger is actuated by a cable-conduit system routed through two or three mechanical springs that act as both the structure and the moving elements (joints) of the hand. Each flexible element will translate and rotate (flex) while actuated by a single cable-conduit mechanism, that transfers the linear force into lateral and axial deflection. This configuration is similar to that of the flexor tendons in the human hand.

The IOWA hand is composed of five active fingers, each capable of bending at the metacarpo-phalangeal (MCP), proximal interphalangeal (PIP) and distal interphalangeal (DIP) joints. These joints offer low-friction bending while resisting lateral deflection. With three joints in each finger (Fig. 2), this design represents a significant change from current prosthetic hands that bend at only two MCP joints and at no PIP or DIP joints.

Indeed, most current prosthetic hands only bend at the metacarpo-phalangeal joint in each of the first two fingers. The remaining two fingers are typically passive. Finger flexion, therefore, does not accurately mimic the movement of the human hand. Past designs using multiple phalanges and joints within each finger to improve finger movement have proven disappointing.

Each finger comprises a number of springs, compression links, cables and conduits. Each spring acts as a joint. Affecting a tension force on a cable through the conduit will yield a deformation in the spring, both in transverse and in compression. Compression links act as a connecting holder for the cable and as a restrainer for the conduit as the spring is flexed within. The IOWA hand (Figs. 3 and 4) exhibits significantly lighter weight; with the correct choice of materials, the completed hand prosthesis would weigh at 90 g. This is approximately half of the endoskeletal [7] prosthesis (203 g) and one fourth of the Otto Bock (390 g) and APRL (421 g) hands (shown in Fig. 1) where current hooks made by Hosmer Dorrance including the aluminum model 5XA and stainless steel model 5X weigh 113 and 213 g, respectively.

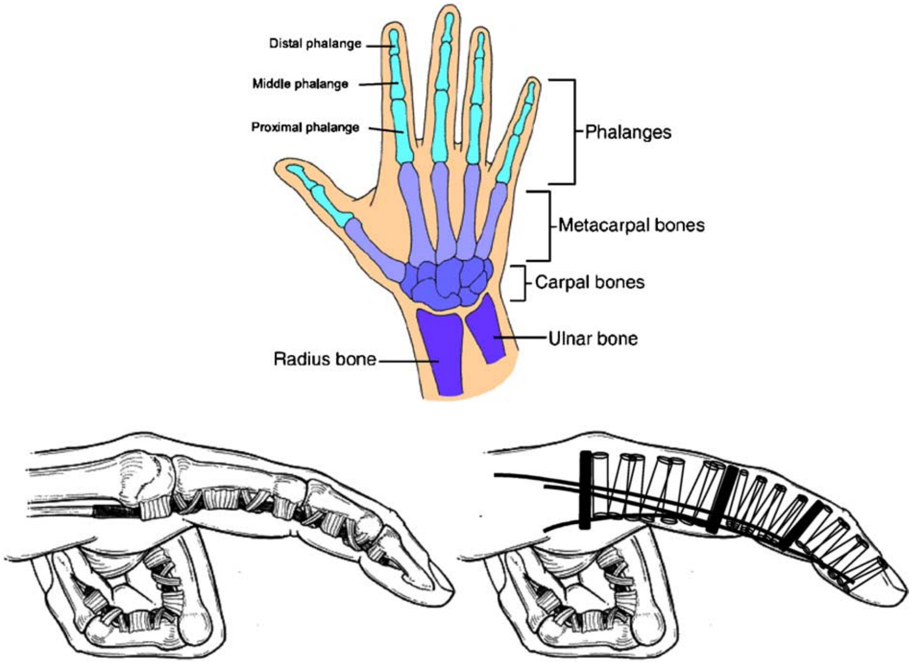

Fig. 2. A schematic of the principles governing the Iowa hand.

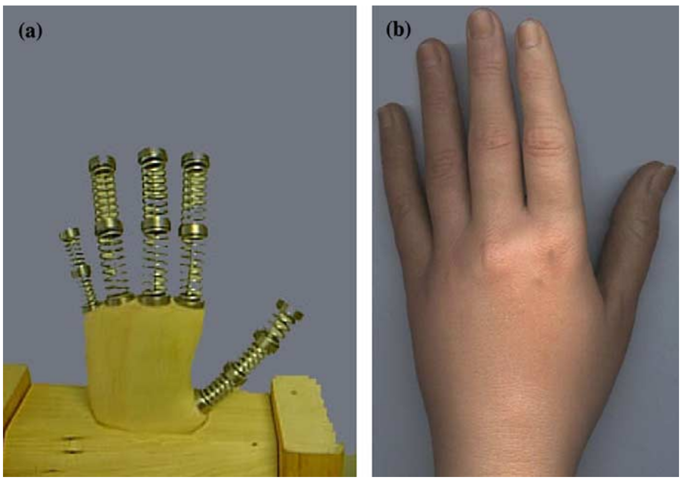

Fig. 3. (a) The IOWA hand—no glove. (b) Hand with cosmetic glove Model 8056 from Linea Orthopedics, AB.

2.1. Advantages and disadvantages of the IOWA hand

The simplistic design of the IOWA hand yields a number of significant benefits to the user. We shall enumerate these benefits in view of preliminary testing. More rigorous testing will be conducted over a period of two years.

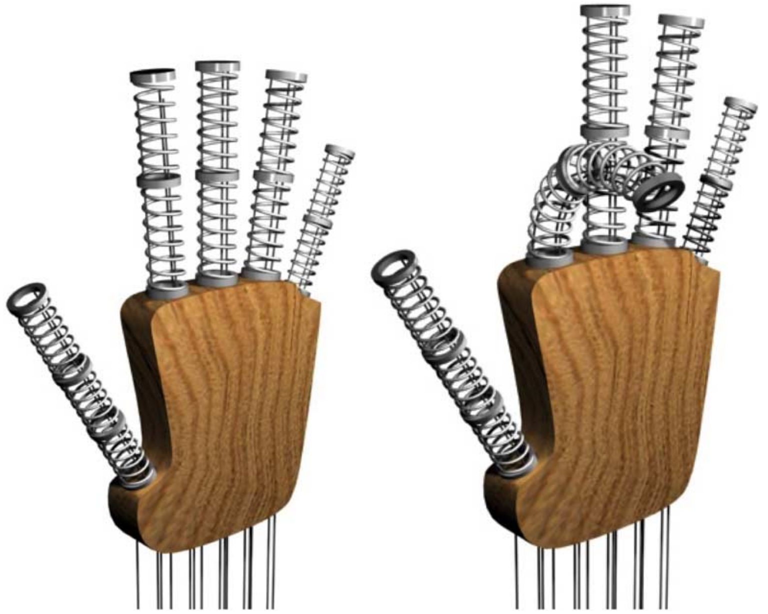

Fig. 4. Prototype of the IOWA prosthesis.

(a) *Actuators can be mounted elsewhere on the body (not on the arm):* The cable-conduit system (similar to that used in the brake system of a bicycle), allows for remote actuation of the spring element. As a result, the actuators are located elsewhere, typically on a belt around the waist.
(b) *Adjustable grasps and dexterity:* The modular design of the hand allows for various angles on each finger and at each joint. Human anatomy allows for grasping complex geometry using intricate coordinated control of the five fingers. To avoid such a control scheme, it was deemed preferable to allow for a variable adjustable angle at the base of each compression link as shown in Fig. 5.
(c) *Realistic finger movement:* Given the adjustable compliance of the hand and given unique design parameters consistent with the user's anthropometric measures, the hand will perform with great fidelity (Fig. 6). While our preliminary testing has shown a significant improvement over other such mechanisms, design of several hands to match several patients will be accomplished and tested over the next few years.
(d) *Inherently compliant:* As a human hand is not rigid, but allows for great flexibility when in the relaxed condition, and some flexibility in the tight condition, the IOWA hand provides adequate compliance. Stiffness/compliance characteristics are adjustable to fit the user's preference and will be addressed in greater detail in the following section.
(e) *Force transmission ratio is high which allows pinch force at the fingertips:* The cable-conduit system provides good transmission ratio between the actuator and the hand. Pinch force at the fingertips is achieved, however, fine control over motion between two fingers is difficult to attain and requires practice.

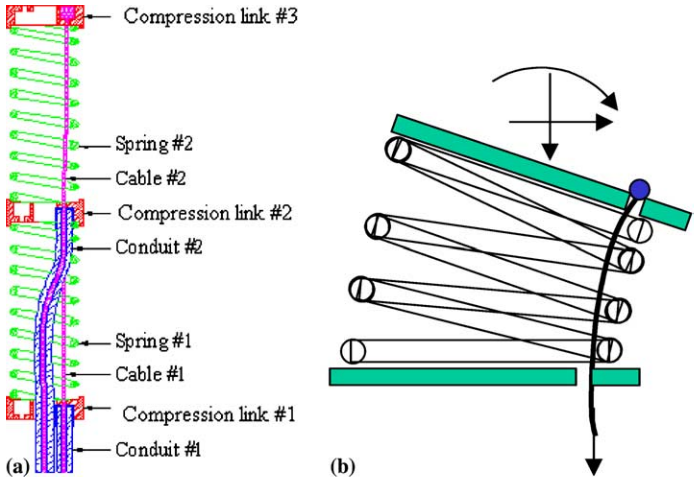

Fig. 5. Adjustable angles of the compression link: (a) schematic of a finger (two joints) and (b) motion of a joint.

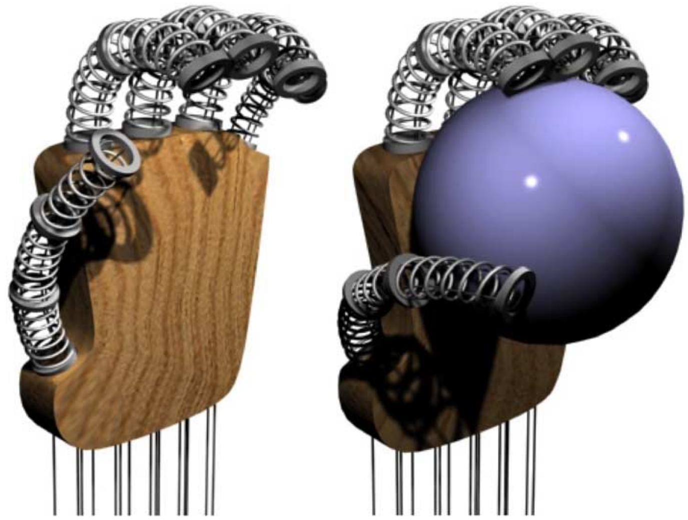

Fig. 6. IOWA hand prosthesis (grasping one object).

(f) *Good cosmetic characteristics:* With a commercial cosmetic glove, the IOWA hand exhibits acceptable esthetics. The first and only hand designed by this group matches the size of an adult male. Many other considerations must be addressed if a hand is to be designed for a female or a child, in particular, the strength to weight ratio, actuator forces, compliance and weight.

(g) *Joint independent actuation:* Flexing of each spring element is independently controlled. This allows the user to manipulate each segment, but also allows the control system to introduce coupling between the PIP and DIP as is the case in a normal hand.

3. Analysis of the IOWA hand

In order to consider the spring behaving like an elastic rod, its rigidity in bending is written as

$$K_b = -\frac{B}{d\varphi/du} = \frac{Ed^4L}{32nD\left(1+\frac{E}{2G}\right)} \tag{1a}$$

where B is the moment, and $d\varphi/du$ is bending rotation angle for the element length du, E and G are the material elastic normal and tangential modula, respectively, n is the number of active coils, d is the wire diameter, D is the mean spring diameters, L is the length of the loaded spring and φ is the bending rotation angle.

Rigidity in shear is defined as

$$K_s = \frac{S}{\phi} = \frac{Ed^4L}{8nD^3} \tag{1b}$$

where S is the shear load, and ϕ is the shear angle.

Rigidity in compression as

$$K = \frac{V}{\delta_a} = \frac{Gd^4}{8nD^3} \tag{1c}$$

where V is the axial load, δ_a is the axial displacement.

Rigidity in coupling as

$$K_{sb} = \frac{Ed^4}{64nD} \tag{1d}$$

3.1. Haringx element method

The basic concept is the division of the spring into small elements consisting of ordinary, linear springs. The unloaded length of the element I (Fig. 7) is Δl_0, the internal forces for the two end nodes are shear forces T_{i-1} and T_i, axial forces V_{i-1} and V_i, moments M_{i-1} and M_i. Utilizing

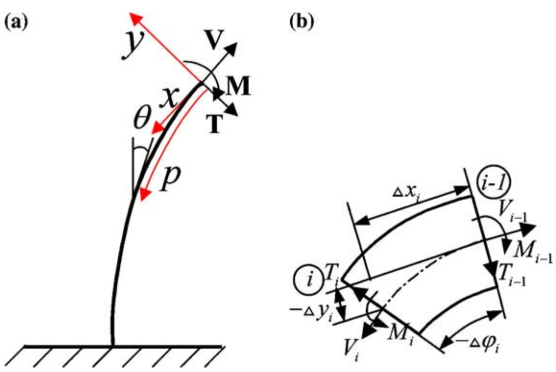

Fig. 7. The Haringx model of the helical spring: (a) center line of the loaded spring and (b) element I.

equilibrium as presented by Lindkvist [23] the distance Δx_i and Δy_i, and rotation, $\Delta\varphi_i$ are obtained between the two end nodes (i) and $(i-1)$ as

$$\Delta x_i = \Delta l_0 + \frac{V_{i-1}}{K_i} \tag{2a}$$

$$\Delta\varphi_i = -\frac{M_{i-1}K_{\mathrm{b},i} + T_{i-1}K_{\mathrm{s},i}}{(K_{\mathrm{s},i} - \Delta x_i K_{\mathrm{sb},i})K_{\mathrm{b},i} + K_{\mathrm{sb},i}^2} \tag{2b}$$

$$\Delta y_i = \frac{T_{i-1} + \Delta\varphi_i K_{\mathrm{sb},i}}{K_{\mathrm{b},i}} \tag{2c}$$

where $K_{\mathrm{b},i}$, K_s, $K_{\mathrm{sb},i}$ and K_i are the rigidities of bending, shear, coupling and compression for element I respectively. The total displacement from the upper end to end (i) is now obtained by

$$x_i = x_{i-1} + \Delta x_{i-1}\cos\varphi_{i-1} - \Delta y_{i-1}\sin\varphi_{i-1} \tag{3a}$$

$$y_i = y_{i-1} + \Delta y_{i-1}\cos\varphi_{i-1} + \Delta x_{i-1}\sin\varphi_{i-1} \tag{3b}$$

$$\varphi_i = \varphi_{i-1} + \Delta\varphi_i \tag{3c}$$

The load to the next element is

$$V_i = V\cos\varphi_i + T\sin\varphi_i \tag{4a}$$

$$T_i = T\cos\varphi_i - V\sin\varphi_i \tag{4b}$$

$$M_i = M + Tx_i - Vy_i \tag{4c}$$

and the deflection of the next element can be calculated using Eq. (4) and repeating this procedure for all elements up to the final element one obtains the deformation of the fixed end with respect to the free end.

Fig. 8 shows the relationship between three coordinate systems. Therefore after we obtain x, y and φ, the deformation of the fixed end with respect to the free end the relations between the three systems are

$$\begin{Bmatrix} x_1 \\ y_1 \end{Bmatrix} = \begin{bmatrix} 0 & 1 \\ -1 & 0 \end{bmatrix} \begin{Bmatrix} x \\ y \end{Bmatrix} \tag{5a}$$

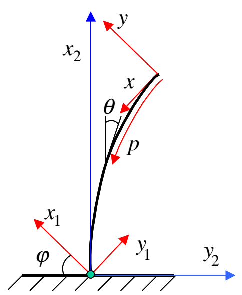

Fig. 8. The relationship of three coordinate systems.

$$\begin{Bmatrix} x_2 \\ y_2 \end{Bmatrix} = \begin{bmatrix} \cos\left(\frac{\pi}{2}-\varphi\right) & -\sin\left(\frac{\pi}{2}-\varphi\right) \\ \sin\left(\frac{\pi}{2}-\varphi\right) & \cos\left(\frac{\pi}{2}-\varphi\right) \end{bmatrix} \begin{Bmatrix} x_1 \\ y_1 \end{Bmatrix} \tag{5b}$$

where $[x \quad y]^{\mathrm{T}}$ is the position vector of point O in system $x-y$, $[x_1 \quad y_1]^{\mathrm{T}}$ is the position vector of free end in system x_1-y_1, $[x_2 \quad y_2]^{\mathrm{T}}$ is the position vector of free end in system x_2-y_2, φ is the rotation angle of fixed end in system $x-y$, and φ_2 is the free end rotation angle in system x_2-y_2.

From Eq. (5) one can obtain

$$\begin{Bmatrix} x_2 \\ y_2 \end{Bmatrix} = \begin{bmatrix} \sin\left(\frac{\pi}{2}-\varphi\right) & \cos\left(\frac{\pi}{2}-\varphi\right) \\ -\cos\left(\frac{\pi}{2}-\varphi\right) & \sin\left(\frac{\pi}{2}-\varphi\right) \end{bmatrix} \begin{Bmatrix} x \\ y \end{Bmatrix} \tag{6}$$

and

$$\varphi_2 = \varphi \tag{7}$$

The final deflection in the x_2oy_2 system is

$$\mathrm{d}x = L - x\sin\left(\frac{\pi}{2}-\varphi\right) - y\sin\left(\frac{\pi}{2}-\varphi\right) \tag{8a}$$

$$\mathrm{d}y = y\sin\left(\frac{\pi}{2}-\varphi\right) - y\cos\left(\frac{\pi}{2}-\varphi\right) \tag{8b}$$

$$\varphi_2 = \varphi \tag{8c}$$

Because we also need the stiffness matrix, a transformation matrix from one coordinate system to another must be developed. In Fig. 9 consider the spring with the generalized coordinates $\mathbf{q} = [x \quad y \quad \varphi]^{\mathrm{T}}$ and load $\mathbf{Q} = [V \quad T \quad M]^{\mathrm{T}}$. Apply the small changes in the load $\pm\delta\mathbf{Q}$ and use the Haringx method to calculate $\mathbf{q}(\mathbf{Q}+\delta\mathbf{Q})$ and $\mathbf{q}(\mathbf{Q}-\delta\mathbf{Q})$, then

$$\delta\mathbf{q} = \frac{1}{2}[\mathbf{q}(\mathbf{Q}+\delta\mathbf{Q}) - \mathbf{q}(\mathbf{Q}-\delta\mathbf{Q})] \tag{9}$$

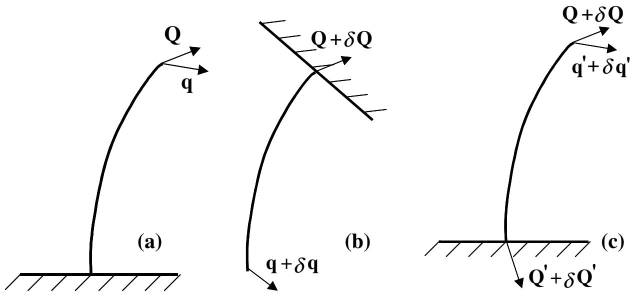

Fig. 9. Deformation transformation: (a) spring with generalized coordinates and load, (b) loaded at the upper end and deformation at the lower end, (c) deformation at the upper end and with the lower end fixed and the load at both ends.

We perform three different and linearly independent changes to obtain

$$\begin{bmatrix} \delta V_1 & \delta V_2 & \delta V_3 \\ \delta T_1 & \delta T_2 & \delta T_3 \\ \delta M_1 & \delta M_2 & \delta M_3 \end{bmatrix} = \mathbf{S} \begin{bmatrix} \delta x_1 & \delta x_2 & \delta x_3 \\ \delta y_1 & \delta y_2 & \delta y_3 \\ \delta \varphi_1 & \delta \varphi_2 & \delta \varphi_3 \end{bmatrix} \tag{10}$$

From Eq. (10) we can solve for $\mathbf{S}$ as

$$\mathbf{S} = \begin{bmatrix} \delta V_1 & \delta V_2 & \delta V_3 \\ \delta T_1 & \delta T_2 & \delta T_3 \\ \delta M_1 & \delta M_2 & \delta M_3 \end{bmatrix} \begin{bmatrix} \delta x_1 & \delta x_2 & \delta x_3 \\ \delta y_1 & \delta y_2 & \delta y_3 \\ \delta \varphi_1 & \delta \varphi_2 & \delta \varphi_3 \end{bmatrix}^{-1} \tag{11}$$

$$\delta \mathbf{Q}' = \mathbf{S}^{\mathrm{T}} \delta \mathbf{q}' \tag{12}$$

$$\delta \mathbf{Q} = \mathbf{S}' \delta \mathbf{d}' \tag{13}$$

where

$$\mathbf{S}' = \begin{bmatrix} s_{11} & s_{21} & s_{31} \\ s_{12} & s_{22} & s_{32} \\ s_{11}y - s_{12}x - s_{13} - T & s_{21}y - s_{22}x - s_{23} + V & s_{31}y - s_{32}x - s_{33} \end{bmatrix}$$

x and y are the distance between the two ends, $\mathbf{S}'$ is the stiffness matrix for Haringx model.

Eqs. (8) present a simple deflection model of the planar motion of each segment. In order to enable the calculation of spatial deflection, we further develop an element stiffness model.

3.2. Element stiffness model

The linear load–deformation relationship for a small element of the helical spring will first be established. There are two coordinate systems, global system denoted by *abc* and local system denoted by *xyz*. The *a*-axis is along the center line of the undeformed element. The *x*-axis is along the center line of the wire. The *y*-axis is perpendicular to the *a*-axis as shown in Fig. 10. The external load is $\mathbf{F} = [F_a \quad F_b \quad F_c]^{\mathrm{T}}$ and $\mathbf{M} = [M_a \quad M_b \quad M_c]^{\mathrm{T}}$ at the bottom center point of the top knuckle. The pitch angle is defined by $\eta = \arctan(\frac{L}{n\pi D})$.

For one element in Fig. 10 the rotational angle ϕ with respect to the *a*-axis changes from ϕ_1 to ϕ_2. The internal forces and moments at the local coordinate system *xyz* are obtained using the following transformations:

(a) translating the action of the force along the global *a*-axis;
(b) rotating it to the direction of the local *y*-axis;
(c) translating it along the local *y*-axis;
(d) rotating it the pitch angle about the local *y*-axis.

Therefore the internal forces and moments can now be expressed as the multiplication of the associated transformation matrices as follows:

$$\mathbf{Q}_{xyz} = \mathbf{R}_{\eta} \mathbf{U}_y \mathbf{R}_{\phi} \mathbf{U}_a \mathbf{Q}_{abc} \tag{14}$$

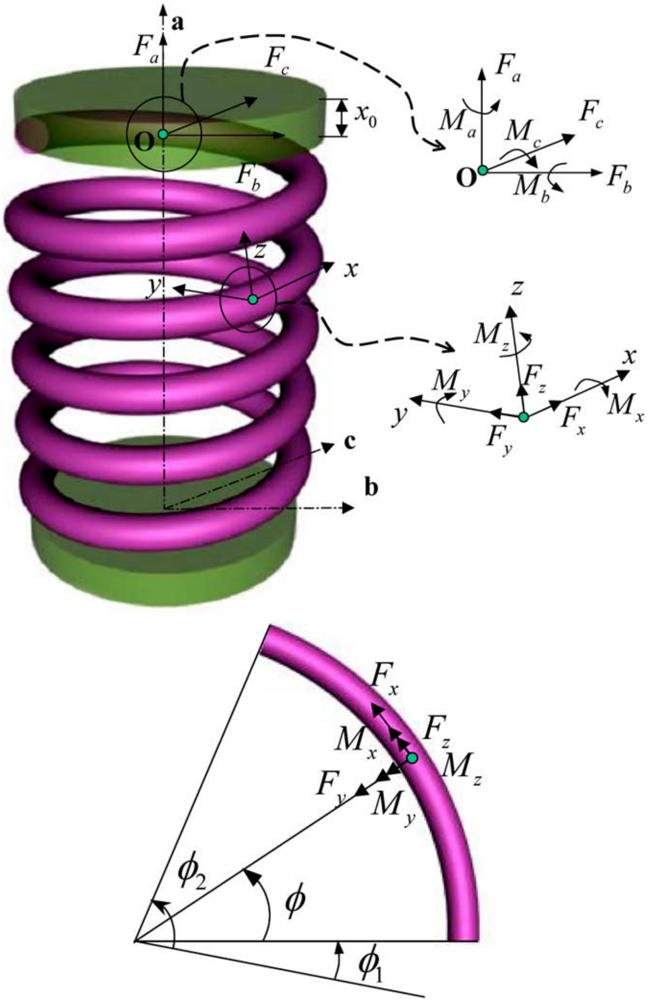

Fig. 10. The spring element and the coordinate systems.

where $\mathbf{Q}_{xyz} = [F_x \quad F_y \quad F_z \quad M_x \quad M_y \quad M_z]^{\mathrm{T}}$, $\mathbf{Q}_{abc} = [F_a \quad F_b \quad F_c \quad M_a \quad M_b \quad M_c]^{\mathrm{T}}$, and where each matrix is defined as follows:

$$\mathbf{R}_\eta = \begin{bmatrix} \cos\eta & 0 & \sin\eta & 0 & 0 & 0 \\ 0 & 1 & 0 & 0 & 0 & 0 \\ -\sin\eta & 0 & \cos\eta & 0 & 0 & 0 \\ 0 & 0 & 0 & \cos\eta & 0 & \sin\eta \\ 0 & 0 & 0 & 0 & 1 & 0 \\ 0 & 0 & 0 & -\sin\eta & 0 & \cos\eta \end{bmatrix}, \quad \mathbf{U}_y = \begin{bmatrix} 1 & 0 & 0 & 0 & 0 & 0 \\ 0 & 1 & 0 & 0 & 0 & 0 \\ 0 & 0 & 1 & 0 & 0 & 0 \\ 0 & 0 & \frac{D}{2} & 1 & 0 & 0 \\ 0 & 0 & 0 & 0 & 1 & 0 \\ -\frac{D}{2} & 0 & 0 & 0 & 0 & 1 \end{bmatrix}$$

$$\mathbf{R}_\phi = \begin{bmatrix} 0 & \sin\phi & \cos\phi & 0 & 0 & 0 \\ 0 & -\cos\phi & \sin\phi & 0 & 0 & 0 \\ 0 & 0 & 1 & 0 & 0 & 0 \\ 0 & 0 & 0 & 0 & \sin\phi & \cos\phi \\ 0 & 0 & 0 & 0 & -\cos\phi & \sin\phi \\ 0 & 0 & 0 & 0 & 0 & 1 \end{bmatrix}$$

$$\mathbf{U}_a = \begin{bmatrix} 1 & 0 & 0 & 0 & 0 & 0 \\ 0 & 1 & 0 & 0 & 0 & 0 \\ 0 & 0 & 1 & 0 & 0 & 0 \\ 0 & 0 & 0 & 1 & 0 & 0 \\ 0 & 0 & \frac{D(\phi_2-\phi)}{2}\tan\eta & 0 & 1 & 0 \\ 0 & -\frac{D(\phi_2-\phi)}{2}\tan\eta & 0 & 0 & 0 & 1 \end{bmatrix}$$

The elastic energy of the curved beam between angles ϕ_1 and ϕ_2 is defined by Lindkvist [23]

$$U = \int_{\phi_1}^{\phi_2} \left[\frac{\left(F_x + \frac{2M_z}{1+(\tan\eta)^2}\right)^2}{2EA} + \frac{F_y^2}{2kGA} + \frac{M_z^2}{2EJ} + \frac{M_x^2}{2GK} + \frac{F_x^2}{2kGA} + \frac{M_y^2}{2EI} \right] \frac{D}{2\cos\eta} \mathrm{d}\phi \tag{15}$$

where

$$J = \frac{\pi D^4}{8}\left(1 - \frac{1}{2}\left(\frac{d}{D}\right)^2 - \sqrt{1-\left(\frac{d}{D}\right)^2}\right) \quad \text{and} \quad K = \left(1 + \frac{3\left(\frac{d}{D(1+(\tan\eta)^2)}\right)^2}{16\left(1-\frac{d}{D(1+(\tan\eta)^2)}\right)^2}\right)\frac{\pi d^4}{32}$$

$$F_x = F_c\cdot\cos\eta\cdot\cos\phi + F_a\cdot\sin\eta + F_b\cdot\cos\eta\cdot\sin\phi \tag{16a}$$

$$F_y = -F_b\cdot\cos\phi + F_c\cdot\sin\phi \tag{16b}$$

$$F_z = F_a\cdot\cos\eta - F_c\cdot\cos\phi\cdot\sin\eta - F_b\cdot\sin\eta\cdot\sin\phi \tag{16c}$$

$$\begin{aligned} M_x = {} & \frac{D}{2}F_a\cdot\cos\eta + M_c\cdot\cos\eta\cdot\cos\phi + M_a\cdot\sin\eta + M_b\cdot\cos\eta\cdot\sin\phi \\ & + F_b\left(-\frac{D}{2}(\phi_2-\phi)\cdot\cos\phi\cdot\sin\eta - \frac{D}{2}\sin\eta\cdot\sin\phi\right) \\ & + F_c\left(\frac{D}{2}(\phi_2-\phi)\cdot\sin\phi\cdot\sin\eta - \frac{D}{2}\sin\eta\cdot\cos\phi\right) \end{aligned} \tag{16d}$$

$$\begin{aligned} M_y = {} & -M_b\cdot\cos\phi + M_c\cdot\sin\phi - \frac{D}{2}F_c(\phi_2-\phi)\cdot\cos\phi\cdot\tan\eta \\ & - \frac{D}{2}F_b(\phi_2-\phi)\cdot\sin\phi\cdot\tan\eta \end{aligned} \tag{16e}$$

$$M_z = M_a \cos\eta - \frac{D}{2} F_a \cdot \sin\eta - M_c \cos\phi \cdot \sin\eta - M_b \sin\eta \cdot \sin\phi + F_b \left(-\frac{D}{2}\cos\eta \cdot \sin\phi + \frac{D}{2}(\phi_2 - \phi)\cos\phi \cdot \sin\eta \cdot \tan\eta \right) + F_c \left(-\frac{D}{2}\cos\eta \cdot \cos\phi - \frac{D}{2}(\phi_2 - \phi)\sin\phi \cdot \sin\eta \cdot \tan\eta \right) \quad (16f)$$

Using the Castigliano theorem the deformation at the end of the element is

$$\delta d_a^e = \frac{\partial U}{\partial F_a}, \quad \delta d_b^e = \frac{\partial U}{\partial F_b}, \quad \delta d_c^e = \frac{\partial U}{\partial F_c}, \quad \delta\varphi_a^e = \frac{\partial U}{\partial M_a}, \quad \delta\varphi_b^e = \frac{\partial U}{\partial M_b}, \quad \delta\varphi_c^e = \frac{\partial U}{\partial M_c}$$

and if we write in matrix form $\mathbf{q}_{abc}^e = H\mathbf{Q}_{abc}^e$, where $H_{6\times6}$ is the element stiffness matrix whose elements are listed in Appendix A.

The element stiffness matrix obtained characterizes the relationship between changes in load at the free end and changes in displacement of the lower end. The desired relationship is between the load and displacement at the free end of the spring. Therefore it needs some transformations. Consider the spring in Fig. 9 with the generalized load $\mathbf{Q}_1 + \delta\mathbf{Q}_1$ at the free end where the preload is $\mathbf{Q}_1$ and there is a small increment $\delta\mathbf{Q}_1$. According to the equilibrium the corresponding load at the fixed end is $\mathbf{Q}_2 + \delta\mathbf{Q}_2$. We have $\delta\mathbf{Q}_1 = \mathbf{S}_{12}\delta\mathbf{q}_2$, where $\mathbf{S}_{12}$ is the stiffness matrix (Fig. 11). We also can obtain the relationship between $\delta\mathbf{Q}_2$ and $\delta\mathbf{q}_1$ by

$$\delta\mathbf{Q}_2 = \mathbf{S}_{12}^{\mathrm{T}}\delta\mathbf{q}_1 \quad (17)$$

According to equilibrium one can derive

$$\mathbf{Q}_2 + \delta\mathbf{Q}_2 = \mathbf{U}_{\mathbf{r}+\delta\mathbf{r}}(\mathbf{Q}_1 + \delta\mathbf{Q}_1) = (\mathbf{U}_\mathbf{r} + \delta\mathbf{U}_\mathbf{r})(\mathbf{Q}_1 + \delta\mathbf{Q}_1) \quad (18)$$

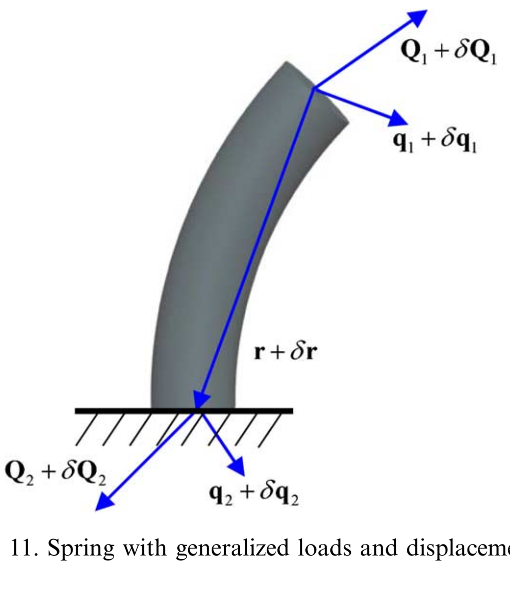

Fig. 11. Spring with generalized loads and displacements.

where $\delta\mathbf{U_r} = \begin{bmatrix} \mathbf{0} & \mathbf{0} \\ \delta\tilde{\mathbf{r}} & \mathbf{0} \end{bmatrix}_{6\times 6}$, $\mathbf{U_r}$ is the transformation matrix for translation, and $\delta\tilde{\mathbf{r}}$ is a 3×3 skew-symmetric matrix.

From Eq. (18) expanding the parentheses yields

$$\mathbf{Q}_2 + \delta\mathbf{Q}_2 = \mathbf{U_r}\mathbf{Q}_1 + \delta\mathbf{U_r}\mathbf{Q}_1 + \mathbf{U_r}\delta\mathbf{Q}_1 + \delta\mathbf{U_r}\delta\mathbf{Q}_1 \tag{19}$$

substitute $\mathbf{Q}_2 = \mathbf{U_r}\mathbf{Q}_1$ into Eq. (19) yields

$$\delta\mathbf{Q}_2 = \delta\mathbf{U_r}\mathbf{Q}_1 + \mathbf{U_r}\delta\mathbf{Q}_1 + \delta\mathbf{U_r}\delta\mathbf{Q}_1 \tag{20}$$

Neglecting terms of higher order yields

$$\delta\mathbf{Q}_1 = \mathbf{U_r}^{-1}(\delta\mathbf{Q}_2 - \delta\mathbf{U_r}\mathbf{Q}_1) \tag{21}$$

From Eq. (18) we can obtain

$$\delta\mathbf{U_r}\mathbf{Q}_1 = \begin{bmatrix} \mathbf{0} & \mathbf{0} \\ \delta\tilde{\mathbf{r}} & \mathbf{0} \end{bmatrix}\mathbf{Q}_1 = \begin{bmatrix} \mathbf{0} & \mathbf{0} \\ \delta\tilde{\mathbf{r}}\mathbf{F}_1 & \mathbf{0} \end{bmatrix} = -\begin{bmatrix} \mathbf{0} & \mathbf{0} \\ \delta\tilde{\mathbf{F}}_1\mathbf{r} & \mathbf{0} \end{bmatrix} \approx -\begin{bmatrix} \mathbf{0} & \mathbf{0} \\ \tilde{\mathbf{F}}_1 & \mathbf{0} \end{bmatrix}\delta\mathbf{q}_1 \tag{22}$$

From Eqs. (17), (20) and (21)

$$\delta\mathbf{Q}_1 = \mathbf{U_r}^{-1}\left(\mathbf{S}_{12}^{\mathrm{T}}\delta\mathbf{q}_1 + \begin{bmatrix} \mathbf{0} & \mathbf{0} \\ \tilde{\mathbf{F}}_1 & \mathbf{0} \end{bmatrix}\delta\mathbf{q}_1\right) \tag{23}$$

Therefore

$$\mathbf{S}_{11} = \mathbf{U_r}^{-1}\left(\mathbf{S}_{12}^{\mathrm{T}} + \begin{bmatrix} \mathbf{0} & \mathbf{0} \\ \tilde{\mathbf{F}}_1 & \mathbf{0} \end{bmatrix}\right) \tag{24}$$

where $\mathbf{S}_{11}$ is the stiffness matrix.

The deflection obtained above characterizes the displacement of the fixed end with respect to the free end resolved in the $\mathbf{x}_1\mathbf{y}_1\mathbf{z}_1$ system. Therefore, it is now necessary to transform it to the coordinate system $\mathbf{xyz}$ in Fig. 12(a). Indeed, the system $\mathbf{x}_1\mathbf{y}_1\mathbf{z}_1$ is a local coordinate system at the free end of the spring; the system $\mathbf{x}_2\mathbf{y}_2\mathbf{z}_2$ is another local coordinate system, which locates at the fixed end, coincides with the origin O of the global coordinate system $\mathbf{xyz}$ and has the same orientation of the system $\mathbf{x}_1\mathbf{y}_1\mathbf{z}_1$. The vector $\mathbf{r} = [x \quad y \quad z]^{\mathrm{T}}$ is defined in $\mathbf{xyz}$ system. Angles α, β and γ from the element stiffness model are the deflection angles (Euler's angles) at the fixed end in $\mathbf{x}_1\mathbf{y}_1\mathbf{z}_1$ system.

From $\mathbf{x}_1\mathbf{y}_1\mathbf{z}_1$ to $\mathbf{x}_2\mathbf{y}_2\mathbf{z}_2$

$$[x_2 \quad y_2 \quad z_2]^{\mathrm{T}} = -[x_1 \quad y_1 \quad z_1]^{\mathrm{T}} \tag{25}$$

The relationship between the two coordinate system $\mathbf{x}_2\mathbf{y}_2\mathbf{z}_2$ and $\mathbf{xyz}$ can be defined by

$$\mathbf{r}_{\mathbf{x}_2\mathbf{y}_2\mathbf{z}_2} = \mathbf{R}\mathbf{r}_{\mathbf{xyz}} \tag{26}$$

where

$$\mathbf{R} = \begin{bmatrix} \cos\beta\cos\gamma & -\cos\beta\sin\gamma & \sin\beta \\ \cos\alpha\sin\gamma + \sin\alpha\sin\beta\cos\gamma & \cos\alpha\cos\gamma - \sin\alpha\sin\beta\sin\gamma & -\sin\alpha\cos\beta \\ \sin\alpha\sin\gamma - \cos\alpha\sin\beta\cos\gamma & \sin\alpha\cos\gamma + \cos\alpha\sin\beta\sin\gamma & \cos\alpha\cos\beta \end{bmatrix} \tag{27}$$

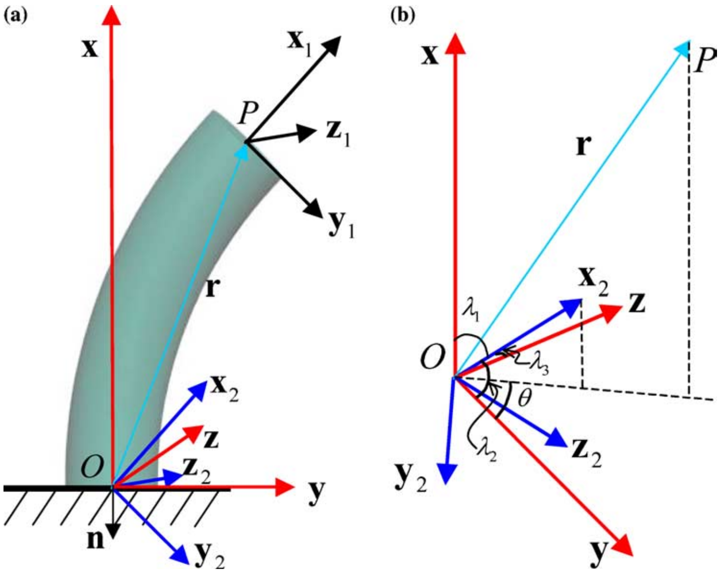

Fig. 12. Coordinate systems: (a) the relationship of three systems and (b) **xyz** and $\mathbf{x}_2\mathbf{y}_2\mathbf{z}_2$.

Assume the unit vector $\mathbf{x}_2 = [\cos\lambda_1 \quad \cos\lambda_2 \quad \cos\lambda_3]^{\mathrm{T}}$ and the relationship is shown in Fig. 12(b). Therefore, we have the following equations from Fig. 12(b)

$$(\cos\lambda_1)^2 + (\cos\lambda_2)^2 + (\cos\lambda_3)^2 = 1 \tag{28a}$$

$$\cos\lambda_3 = \tan\theta\cos\lambda_2 \tag{28b}$$

$$\tan\theta = \frac{z}{y} \tag{28c}$$

$$\lambda_1 = \alpha \tag{28d}$$

The position vector of the free end can be represented in **xyz** by

$$\begin{Bmatrix} x \\ y \\ z \end{Bmatrix} = \begin{Bmatrix} -x_1\cos\beta\cos\gamma - x_3\sin\beta + x_2\cos\beta\sin\gamma \\ x_3\cos\beta\sin\alpha - x_1(\cos\gamma\sin\alpha\sin\beta + \cos\alpha\sin\gamma) - x_2(\cos\alpha\cos\gamma - \sin\alpha\sin\beta\sin\gamma) \\ -x_3\cos\beta\cos\alpha - x_1(-\cos\alpha\cos\gamma\sin\beta + \sin\alpha\sin\gamma) - x_2(\sin\alpha\cos\gamma + \cos\alpha\sin\beta\sin\gamma) \end{Bmatrix} \tag{29}$$

The final deflection of the free end with respect to the fixed end is defined by

$$\Delta x = L - x \tag{30a}$$

where Δx is the deflection in x direction.

$$\Delta y = y \tag{30b}$$

where Δy is the deflection in x direction.

$$\Delta z = z \tag{30c}$$

where Δz is the deflection in z direction.

The three rotation angles are derived as

$$\lambda_1 = \alpha \tag{30d}$$

$$\lambda_2 = \mathrm{Arc}\cos\left(\sqrt{\frac{1-(\cos\alpha)^2}{1+(z/y)^2}}\right) \tag{30e}$$

$$\lambda_3 = \mathrm{Arc}\cos\left(\frac{z}{y}\cos\lambda_2\right) \tag{30f}$$

Eqs. (30) characterize the resulting motion after applying a force through the cable-conduit to move the upper compression link.

4. Implementation

In this section, we implement the deformation equations where mechanical properties of the spring element are shown in Table 1. Applying the Haringx model the results are in Tables 2 and 3.

From Table 3 one can find that the numerical solutions are matching the experiment one closely.

To run the element stiffness model one can obtain the numerical results and compare them with experiment results in Tables 4–7 as follows, where each table shows that it has different external load in the cable-conduit. The results through numerical and experiment methods are almost the same.

Table 1
The mechanical properties

Wire diameter	$d = 0.0023$ m
Mean spring diameter	$D = 0.034$ m
Number of active coils	$n = 6$
Length of the spring	$L = 0.036$ m
Pitch of the spring	$h = 0.09549$ m
Modulus of elasticity	$E = 210$ GPa
Stiffness of the compression	$K = Gd^4/8nD^3$
Modulus of rigidity	$G = 80$ Gpa

Table 2
The transform in different coordinate systems (Haringx model)

	Original coordinate sys.			x_1oy_1 sys.		
	x (cm)	y (cm)	$\Delta\varphi$ (deg)	x_1 (cm)	y_1 (cm)	$\Delta\varphi$ (deg)
$V = -5$ N, $T = 0$, $M = 0.085$ N m	3.1562	0.3508	11.6366	3.1621	0.2931	11.6366
$V = -8$ N, $T = 0$, $M = 0.136$ N m	2.8765	0.5236	17.9118	2.8981	0.3865	17.9118
$V = -10$ N, $T = 0$, $M = 0.17$ N m	2.6878	0.625	21.864	2.7272	0.4209	21.864
$V = -15$ N, $T = 0$, $M = 0.255$ N m	2.2166	0.8379	31.1207	2.3306	0.4283	31.1207

Table 3
The final deflection at the free end

	Calcul. results			Exper. results		
	Δx_2 (cm)	Δy_2 (cm)	$\Delta\varphi$ (deg)	Δx_2 (cm)	Δy_2 (cm)	$\Delta\varphi$ (deg)
$V = -5$ N, $T = 0$, $M = 0.085$ N m	0.4379	0.2931	11.6366	0.4268	0.2692	11.587
$V = -8$ N, $T = 0$, $M = 0.136$ N m	0.7019	0.3865	17.9118	0.712	0.3903	17.912
$V = -10$ N, $T = 0$, $M = 0.17$ N m	0.8728	0.4209	21.864	0.8549	0.4158	21.768
$V = -15$ N, $T = 0$, $M = 0.255$ N m	1.2694	0.4283	31.1207	1.2567	0.433	31.25

Table 4
$Fx = -6$, $Fy = 0$, $Fz = 0$, $Mx = 0$, $My = -0.051$, $Mz = 0.051$

x_1 (mm)	y_1 (mm)	z_1 (mm)	α (deg)	β (deg)	γ (deg)
−30.7436	2.0649	2.3252	0.6053	6.7361	−6.9521
x (mm)	y (mm)	z (mm)	λ_1 (deg)	λ_2 (deg)	λ_3 (deg)
30.828	1.65422	1.31876	0.6053	89.5267	89.6227
Δx(mm)	Δy (mm)	Δz (mm)	$\Delta\lambda_1$ (deg)	$\Delta\lambda_2$ (deg)	$\Delta\lambda_3$ (deg)
5.172	1.65422	1.31876	0.6053	89.5267	89.6227
Experiment results					
5.100	1.580	1.3213	–	–	–

Table 5
$Fx = -9$, $Fy = 0$, $Fz = 0$, $Mx = 0$, $My = -0.102$, $Mz = 0.051$

x_1 (mm)	y_1 (mm)	z_1 (mm)	α (deg)	β (deg)	γ (deg)
−27.9778	1.935	4.2132	1.0137	12.9897	−6.8182
x (mm)	y (mm)	z (mm)	λ_1 (deg)	λ_2 (deg)	λ_3 (deg)
28.2401	1.35299	2.21735	1.0137	89.472	89.1347
Δx (mm)	Δy (mm)	Δz (mm)	$\Delta\lambda_1$ (deg)	$\Delta\lambda_2$ (deg)	$\Delta\lambda_3$ (deg)
7.7599	1.35299	2.21735	1.0137	89.472	89.1347
Experiment results					
7.7599	1.32	2.18	–	–	–

Table 6
$Fx = -12$, $Fy = 0$, $Fz = 0$, $Mx = 0$, $My = -0.051$, $Mz = 0.153$

x_1 (mm)	y_1 (mm)	z_1 (mm)	α (deg)	β (deg)	γ (deg)
−25.2412	5.4005	2.2603	1.3743	5.8173	−19.3334
x (mm)	y (mm)	z (mm)	λ_1 (deg)	λ_2 (deg)	λ_2 (deg)
25.7042	3.23927	0.439209	1.3743	88.6382	89.8154
dx (mm)	dy (mm)	dz (mm)	$\Delta\lambda_1$ (deg)	$\Delta\lambda_2$ (deg)	$\Delta\lambda_3$ (deg)
10.2958	3.23927	0.439209	1.3743	88.6382	89.8154
Experiment results					
10.11	3.25	0.4423	–	–	–

Table 7
$Fx = -17$, $Fy = 0$, $Fz = 0$, $Mx = 0$, $My = -0.204$, $Mz = 0.085$

x_1 (mm)	y_1 (mm)	z_1 (mm)	α (deg)	β (deg)	γ (deg)
−20.5881	2.7134	6.9985	2.5115	23.6845	−10.8644
x (mm)	y (mm)	z (mm)	λ_1 (deg)	λ_2 (deg)	λ_3 (deg)
21.7962	1.11069	1.97626	2.5115	88.7698	87.8108
Δx (mm)	Δy (mm)	Δz (mm)	$\Delta\lambda_1$ (deg)	$\Delta\lambda_2$ (deg)	λ_3 (deg)
14.2038	1.11069	1.97626	2.5115	88.7698	87.8108
Experiment results					
14.13	1.045	1.899	–	–	–

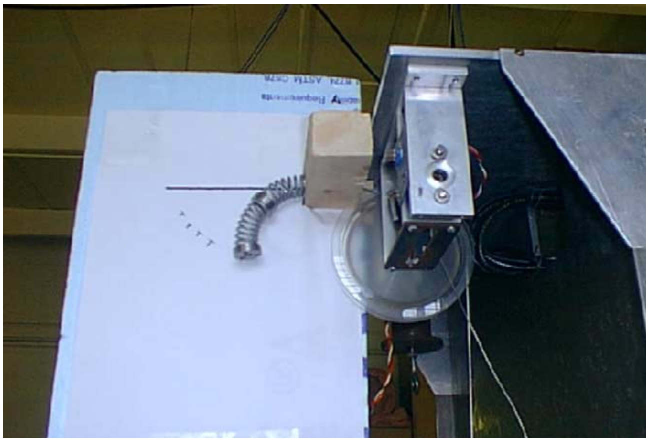

Fig. 13. Experiment setup for a finger of the IOWA hand.

5. Experiment

A mechanism is set up to test the flexing/load relationship for each mechanical spring (Fig. 13). It includes several parts: a pulley, weight block, a frame fixing the base of finger springs. The loads are supplied by different weights through wires in every knuckle. In our experiment we used five different weights: 1, 5, 10, 15 and 20 N. The results are shown in Tables 2–7.

The method of loading the compression spring used in this design induces a lateral deflection with a relative translation and rotation of the upper compression link. Recall that the lower compression link is considered fixed because the motions of the different segments of the finger are independent. This particular aspect of the mechanical spring is what has enabled us to develop a finger-like action, yet maintain the compliant aspect of the hand.

6. Conclusion

The design and analysis of a novel multi-fingered hand has been introduced. It was shown that flexion of a compression spring is implemented as a complex joint in each segmental link of a finger. Five fingers are actuated, each with 3 DOFs. It was shown that loading of a compression spring in both transverse and axial directions and using cable-conduit systems allows for controllable manipulation of the IOWA hand, yet maintains inherent compliance in each finger, a properly that is important to grasping and manipulation. It was shown that the translational motion of the wire through the cable-conduit is transformed into a lateral deflection with a relative translation and rotation of the finger segment. Indeed, this design allows for the location of the actuators far from the hand. It is shown that a Haringx model is used to calculate the solution of the transverse deflection of each finger segment in a general form and an element stiffness model is used to calculate the three dimensional deflection characteristics. Numerical results obtained. The performance of each finger is tested experimentally and compared with the numerical results. Results show that the proposed formulations for predicting planar and spatial deflections using numerical algorithm closely matches experimental results. It is evident that the cost of manufacturing for such a device is relatively low compared with commercial actuated prosthetics.

Appendix A

$$h_{11} = \frac{D\cdot\phi\cdot\sin^6\eta}{2\cdot E\cdot A\cdot\cos\eta} + \frac{D^3\phi\cdot\sin^2\eta}{8\cdot E\cdot J\cdot\cos\eta} + \frac{D^3\phi\cdot\cos\eta}{2\cdot G\cdot K} + \frac{D\cdot\phi\cdot\cos\eta}{k\cdot G\cdot A}$$

$$\begin{aligned} h_{12} = &-\frac{D\cdot\sin^3\eta\cdot(\cos\phi - \cos^2\eta\cdot\cos\phi - \phi\cdot\sin^2\eta\cdot\sin\phi - \sin^2\eta\cdot\cos\phi + \phi_2\cdot\sin^2\eta\cdot\sin\phi)}{2\cdot E\cdot A} \\ &+\frac{D^3\sin\eta\cdot(\phi_2\cdot\sin^2\eta\cdot\sin\phi - \cos^2\eta\cdot\cos\phi - \phi\cdot\sin^2\eta\cdot\sin\phi - \sin^2\eta\cdot\cos\phi)}{8\cdot E\cdot J\cdot\cos^2\eta} \\ &+\frac{D^3\cdot\sin\eta\cdot\sin\phi\cdot(\phi_2-\phi)}{8\cdot G\cdot K} + \frac{D\cdot\sin\eta\cdot\cos\phi}{2\cdot k\cdot G\cdot A} \end{aligned}$$

$$\begin{aligned} h_{13} = &-\frac{D\cdot\sin^3\eta\cdot(\cos^2\eta\cdot\sin\phi + \phi_2\cdot\sin^2\eta\cdot\cos\phi + \sin^2\eta\cdot\sin\phi - \phi\cdot\sin^2\eta\cdot\cos\phi - \sin\phi)}{2\cdot E\cdot A} \\ &+\frac{D^3\sin\eta\cdot(\phi_2\cdot\sin^2\eta\cdot\cos\phi + \cos^2\eta\cdot\sin\phi - \phi\cdot\sin^2\eta\cdot\cos\phi + \sin^2\eta\cdot\sin\phi)}{8\cdot E\cdot J\cdot\cos^2\eta} \\ &+\frac{D^3\cdot\sin\eta\cdot\cos\phi\cdot(\phi_2-\phi)}{8\cdot G\cdot K} - \frac{D\cdot\sin\eta\cdot\cos\phi}{2\cdot k\cdot G\cdot A} \end{aligned}$$

$$h_{14} = \frac{\phi\cdot\cos^2\eta\cdot\sin^3\eta}{E\cdot A} - \frac{D^2\cdot\phi\cdot\sin\eta}{4\cdot E\cdot J} + \frac{D^2\cdot\phi\cdot\sin\eta}{4\cdot G\cdot K}$$

$$h_{15} = \frac{\sin^4\eta\cdot\cos\eta\cdot\cos\phi}{E\cdot A} - \frac{D^2\cdot\sin^2\eta\cdot\cos\phi}{4\cdot E\cdot J\cdot\cos\eta} - \frac{D^2\cdot\cos\eta\cdot\cos\phi}{4\cdot G\cdot K}$$

$$h_{16} = -\frac{\sin^4\eta\cdot\cos\eta\cdot\sin\phi}{E\cdot A} + \frac{D^2\cdot\sin^2\eta\cdot\sin\phi}{4\cdot E\cdot J\cdot\cos\eta} + \frac{D^2\cdot\cos\eta\cdot\sin\phi}{4\cdot G\cdot K}$$

$$h_{21} = -\frac{D \cdot \sin^3 \eta \cdot (\cos \phi - \cos^2 \eta \cdot \cos \phi - \phi \cdot \sin^2 \eta \cdot \sin \phi - \sin^2 \eta \cdot \cos \phi + \phi_2 \cdot \sin^2 \eta \cdot \sin \phi)}{2 \cdot E \cdot A}$$
$$+ \frac{D^3 \sin \eta \cdot (\phi_2 \cdot \sin^2 \eta \cdot \sin \phi - \cos^2 \eta \cdot \cos \phi - \phi \cdot \sin^2 \eta \cdot \sin \phi - \sin^2 \eta \cdot \cos \phi)}{8 \cdot E \cdot J \cdot \cos^2 \eta}$$
$$+ \frac{D^3 \cdot \sin \eta \cdot \sin \phi \cdot (\phi_2 - \phi)}{8 \cdot G \cdot K} + \frac{D \cdot \sin \eta \cdot \cos \phi}{2 \cdot k \cdot G \cdot A}$$

$$h_{24} = -\frac{\cos^3 \eta(\cos \phi - \cos^2 \eta \cdot \cos \phi - \phi \cdot \sin^2 \eta \cdot \sin \phi - \sin^2 \eta \cdot \cos \phi + \phi_2 \cdot \sin^2 \eta \cdot \sin \phi)}{EA}$$
$$- \frac{D^2(\phi_2 \cdot \sin^2 \eta \cdot \sin \phi - \cos^2 \eta \cdot \cos \phi - \phi \cdot \sin^2 \eta \cdot \sin \phi - \sin^2 \eta \cdot \cos \phi)}{4E \cdot J \cdot \cos \eta}$$
$$+ \frac{D^2(\phi_2 - \phi) \sin^2 \eta \cdot \sin \phi}{4G \cdot K \cdot \cos \eta}$$

$$h_{64} = -\frac{2 \cos^4 \eta \cdot \sin \eta \cdot \sin \phi}{D \cdot E \cdot A} - \frac{D \sin \phi \cdot \sin \eta}{2E \cdot J} + \frac{D \sin \phi \cdot \sin \eta}{2G \cdot K}$$

$$h_{65} = -\frac{\sin^2 \eta \cdot \cos^3 \eta \cdot \cos^2 \phi}{D \cdot E \cdot A} - \frac{D \cdot \cos^2 \phi \cdot \sin^2 \eta}{4E \cdot J \cdot \cos \eta} - \frac{D \cdot \cos^2 \phi \cdot \cos \eta}{4G \cdot K} + \frac{D \cos^2 \phi}{4E \cdot I \cdot \cos \eta}$$

$$h_{66} = \frac{\sin^2 \eta \cdot \cos^3 \eta \cdot (\cos \phi \cdot \sin \phi + \phi)}{D \cdot E \cdot A} + \frac{D \cdot (\cos \phi \cdot \sin \phi + \phi) \cdot \sin^2 \eta}{4E \cdot J \cdot \cos \eta}$$
$$+ \frac{D \cdot (\cos \phi \cdot \sin \phi + \phi) \cdot \cos \eta}{4G \cdot K} + \frac{D(\phi - \cos \phi \cdot \sin \phi)}{4E \cdot I \cdot \cos \eta}$$

$$h_{22} = \frac{D \cdot \cos \eta}{24 \cdot E \cdot A}(6\phi - 6 \cdot \cos \phi \cdot \sin \phi + 6 \cdot \phi \cdot \sin^2 \eta - 3 \cdot \phi \cdot \sin^4 \eta + 12 \cdot \cos^2 \eta \cdot \cos \phi \cdot \sin \phi$$
$$+ 6 \cdot \phi_2^2 \cdot \sin^4 \eta \cdot \cos \phi \cdot \sin \phi - 12\phi_2 \cos^2 \eta \cdot \sin^2 \eta \cdot \cos^2 \phi + 12\phi_2 \cdot \sin^2 \eta \cdot \cos^2 \phi$$
$$- 12\phi \cdot \phi_2 \cdot \sin^4 \eta \cdot \cos \phi \cdot \sin \phi - 6\phi^2 \phi_2 \sin^4 \eta + 6\phi_2 \sin^4 \eta \cdot \sin^2 \phi$$
$$+ 12\phi \cdot \cos^2 \eta \cdot \sin^2 \eta \cdot \cos^2 \phi - 6 \cos^2 \eta \cdot \sin^2 \eta \cdot \cos \phi \cdot \sin \phi$$
$$- 6\phi \cdot \cos^2 \eta \cdot \sin^2 \eta - 6 \cos^4 \eta \cdot \cos \phi \cdot \sin \phi - 6\phi \cdot \cos^4 \eta - 12\phi \cdot \cos^2 \eta$$
$$+ 6\phi^2 \cdot \sin^4 \eta \cdot \cos \phi \cdot \sin \phi + 2\phi^3 \cdot \sin^4 \eta + 6\phi \cdot \sin^4 \eta \cdot \cos^2 \phi - 3 \sin^4 \eta \cdot \cos \phi \cdot \sin \phi$$
$$+ 6\phi \cdot \phi_2^2 \cdot \sin^4 \eta - 12\phi \cdot \sin^2 \eta \cdot \cos^2 \phi + 6 \sin^2 \eta \cdot \cos \phi \cdot \sin \phi)$$
$$+ \frac{D^3}{96 \cdot E \cdot J \cdot \cos^3 \eta}(6\phi \cdot \phi_2^2 \cdot \sin^4 \eta - 6 \cdot \cos^4 \eta \cdot \cos \phi \cdot \sin \phi + 6 \cdot \phi_2^2 \cdot \sin^4 \eta \cdot \cos \phi \cdot \sin \phi$$
$$+ 2\phi^3 \cdot \sin^4 \eta + 12\phi \cdot \cos^2 \eta \cdot \sin^2 \eta \cdot \cos^2 \phi - 12 \cdot \phi_2 \cdot \cos^2 \eta \cdot \sin^2 \eta \cdot \cos^2 \phi$$

$$
\begin{aligned}
&- 6\cos^2\eta\cdot\sin^2\eta\cdot\cos\phi\cdot\sin\phi - 6\phi\cdot\sin^2\eta\cdot\cos^2\eta + 6\phi\cdot\cos^4\eta \\
&+ 6\phi^2\cdot\sin^4\eta\cdot\cos\phi\cdot\sin\phi + 6\phi\cdot\sin^4\eta\cdot\cos^2\phi - 3\sin^4\eta\cdot\cos\phi\cdot\sin\phi \\
&- 3\phi\cdot\sin^4\eta - 12\phi\cdot\phi_2^2\cdot\sin^4\eta\cdot\cos\phi\cdot\sin\phi - 6\phi^2\cdot\phi_2\cdot\sin^4\eta + 6\phi_2\cdot\sin^4\eta\cdot\sin^2\phi) \\
&+ \frac{D^3\cdot\sin^2\eta}{96G\cdot K\cdot\cos\eta}(6\phi^2\cdot\sin\phi\cdot\cos\phi - 6\phi\cdot\cos^2\phi + 9\phi - 12\phi\cdot\phi_2\cdot\sin\phi\cdot\cos\phi + 6\phi^2\cdot\sin^2\phi \\
&- 6\phi^2\cdot\phi_2 + 2\phi^3 + 6\phi_2^2\cdot\phi - 3\sin\phi\cdot\cos\phi + 6\phi_2^2\cdot\sin\phi\cdot\cos\phi + 12\phi_2\cdot\cos^2\phi) \\
&+ \frac{D(\sin\phi\cdot\cos\phi + \phi - \sin^2\eta\cdot\cos\phi\cdot\sin\phi + 6\phi\cdot\sin^2\eta)}{4\cdot k\cdot G\cdot A\cdot\cos\eta} \\
&+ \frac{D^3\cdot\sin^2\eta}{96\cdot E\cdot I\cdot\cos^3\eta}(6\phi_2^2\cdot\phi - 6\cdot\phi_2^2\cdot\sin\phi\cdot\cos\phi + 3\sin\phi\cdot\cos\phi - 6\phi^2\cdot\sin\phi\cdot\cos\phi \\
&- 6\phi\cdot\cos^2\phi + 3\phi + 12\phi\cdot\phi_2\cdot\sin\phi\cdot\cos\phi - 6\phi_2\cdot\sin^2\phi - 6\cdot\phi_2\cdot\phi^2 + 2\phi^3)
\end{aligned}
$$

$$
\begin{aligned}
h_{23} = &\frac{D\cdot\cos\eta}{8E\cdot A}(2\phi_2\cdot\sin^4\eta\cdot\cos\phi\cdot\sin\phi - 2\cos^2\phi - 2\cos^4\eta\cdot\cos^2\phi \\
&+ 2\phi_2^2\cdot\sin^4\eta\cdot\cos^2\phi + 4\cos^2\eta\cdot\cos^2\phi - 4\phi\cdot\phi_2\cdot\sin^4\eta\cdot\cos^2\phi \\
&- 2\phi\cdot\sin^4\eta\cdot\cos\phi\cdot\sin\phi - \phi^2\cdot\sin^4\eta - 4\phi\cdot\cos^2\eta\cdot\sin^2\eta\cdot\cos\phi\cdot\sin\phi \\
&+ 2\phi\cdot\phi_2\cdot\sin^4\eta + 2\phi^2\cdot\sin^4\eta\cdot\cos^2\phi + 4\phi\cdot\sin^2\eta\cdot\cos\phi\cdot\sin\phi \\
&+ 4\phi_2\cdot\cos^2\eta\cdot\sin^2\eta\cdot\cos\phi\cdot\sin\phi - 4\phi_2\cdot\sin^2\eta\cdot\cos\phi\cdot\sin\phi + \sin^4\eta\cdot\sin^2\phi \\
&+ 2\sin^2\eta\cdot\cos^2\eta\cdot\sin^2\phi - 2\cdot\sin^2\eta\cdot\sin^2\phi) \\
&+ \frac{D^3}{32E\cdot J\cdot\cos^3\eta}(2\phi^2\cdot\sin^4\eta\cdot\cos^2\phi - 2\phi\cdot\sin^4\eta\cdot\cos\phi\cdot\sin\phi - \phi^2\cdot\sin^4\eta \\
&+ \sin^4\eta\cdot\sin^2\phi + 4\phi_2\cdot\cos^2\eta\cdot\sin^2\eta\cdot\cos\phi\cdot\sin\phi - 2\cos^4\eta\cdot\cos^2\phi \\
&+ 2\phi_2^2\cdot\sin^4\eta\cdot\cos^2\phi - 4\phi\cdot\phi_2\cdot\sin^4\eta\cdot\cos^2\phi + 2\phi_2\cdot\sin^4\eta\cdot\cos\phi\cdot\sin\phi \\
&+ 2\phi\cdot\phi_2\cdot\sin^4\eta - 4\phi\cdot\cos^2\eta\cdot\sin^2\eta\cdot\cos\phi\cdot\sin\phi + 2\cos^2\eta\cdot\sin^2\eta\cdot\sin^2\phi) \\
&+ \frac{D^3\sin^2\eta}{32G\cdot K\cdot\cos\eta}(2\phi_2\cdot\phi - 2\cos^2\phi - 2\phi_2\cdot\cos\phi\cdot\sin\phi - \phi^2 - \sin^2\phi + 2\phi_2^2\cdot\cos^2\phi \\
&+ 2\phi\cdot\cos\phi\cdot\sin\phi + 2\phi^2\cdot\cos^2\phi - 4\phi\cdot\phi_2\cdot\cos^2\phi) + \frac{D\cdot\cos^2\phi\cdot\cos\eta}{4k\cdot G\cdot A} \\
&- \frac{D^3\sin^2\eta}{32E\cdot I\cdot\cos^3\eta}(2\phi^2\cdot\cos^2\phi - 2\phi\cdot\cos\phi\cdot\sin\phi - 4\phi\cdot\phi_2\cdot\cos^2\phi + 2\phi\cdot\phi_2 \\
&+ 2\phi_2\cdot\cos\phi\cdot\sin\phi - \phi^2 + \sin^2\phi + 2\phi_2^2\cdot\cos^2\phi)
\end{aligned}
$$

$$
\begin{aligned}
h_{25} = &-\frac{\cos^2\eta\cdot\sin\eta}{4EA}(2\phi_2\cdot\sin^2\eta\cdot\cos^2\phi + 2\cos^2\eta\cdot\cos\phi\cdot\sin\phi - 2\phi\cdot\cos^2\eta \\
&- 2\phi\cdot\sin^2\eta\cdot\cos^2\phi + \sin^2\eta\cdot\cos\phi\cdot\sin\phi + \phi\cdot\sin^2\eta - 2\cos\phi\cdot\sin\phi + 2\phi)
\end{aligned}
$$

$$
\begin{aligned}
&-\frac{D^2\sin\eta}{16E\cdot J\cdot\cos^2\eta}(\sin^2\eta\cdot\cos\phi\cdot\sin\phi-2\phi\cdot\sin^2\eta\cdot\cos^2\phi+\phi\cdot\sin^2\eta\\
&+2\phi_2\cdot\sin^2\eta\cdot\cos^2\phi+2\cos^2\eta\cdot\cos\phi\cdot\sin\phi-2\phi\cdot\cos^2\eta)\\
&-\frac{D^2\sin\eta(-2\phi\cdot\cos^2\phi-\cos\phi\cdot\sin\phi+3\phi+2\phi_2\cdot\cos^2\phi)}{16G\cdot K}\\
&+\frac{D^2\sin\eta(\phi-2\phi\cdot\cos^2\phi+\cos\phi\cdot\sin\phi+2\phi_2\cdot\cos^2\phi)}{16E\cdot I\cdot\cos^2\eta}
\end{aligned}
$$

$$
\begin{aligned}
h_{26}=&\frac{\cos^2\eta\cdot\sin\eta}{4EA}(-2\phi\cdot\sin^2\eta\cdot\cos\phi\cdot\sin\phi-\phi^2\cdot\sin^2\eta+\sin^2\eta\cdot\sin^2\phi\\
&+2\phi_2\cdot\sin^2\eta\cdot\cos\phi\cdot\sin\phi+2\phi\cdot\phi_2\cdot\sin^2\eta+2\cos^2\phi-2\cos^2\eta\cdot\cos^2\phi)\\
&+\frac{D^2\sin\eta}{16E\cdot J\cdot\cos^2\eta}(-2\phi\cdot\sin^2\eta\cdot\cos\phi\cdot\sin\phi-\phi^2\cdot\sin^2\eta+\sin^2\phi\cdot\sin^2\eta\\
&+2\phi_2\cdot\sin^2\eta\cdot\cos\phi\cdot\sin\phi+2\phi\cdot\phi_2\cdot\sin^2\eta-2\cos^2\phi\cdot\cos^2\eta)\\
&+\frac{D^2\sin\eta(2\cos^2\phi+2\phi_2\cdot\cos\phi\cdot\sin\phi+2\phi\cdot\phi_2+\sin^2\phi-2\phi\cos\phi\cdot\sin\phi-\phi^2)}{16G\cdot K}\\
&+\frac{D^2\sin\eta(2\phi\cdot\phi_2-2\phi_2\cdot\cos\phi\cdot\sin\phi+2\phi\cdot\cos\phi\cdot\sin\phi-\phi^2-\sin^2\phi)}{16E\cdot I\cdot\cos^2\eta}
\end{aligned}
$$

$$
\begin{aligned}
h_{31}=&-\frac{D\cdot\sin^3\eta\cdot(\cos^2\eta\cdot\sin\phi+\phi_2\cdot\sin^2\eta\cdot\cos\phi+\sin^2\eta\cdot\sin\phi-\phi\cdot\sin^2\eta\cdot\cos\phi-\sin\phi)}{2\cdot E\cdot A}\\
&+\frac{D^3\sin\eta\cdot(\phi_2\cdot\sin^2\eta\cdot\cos\phi+\cos^2\eta\cdot\sin\phi-\phi\cdot\sin^2\eta\cdot\cos\phi+\sin^2\eta\cdot\sin\phi)}{8\cdot E\cdot J\cdot\cos^2\eta}\\
&+\frac{D^3\cdot\sin\eta\cdot\cos\phi\cdot(\phi_2-\phi)}{8\cdot G\cdot K}-\frac{D\cdot\sin\eta\cdot\cos\phi}{2\cdot k\cdot G\cdot A}
\end{aligned}
$$

$$
\begin{aligned}
h_{63}=&\frac{\cos^2\eta\cdot\sin\eta}{4EA}(-2\cos\phi\cdot\sin\phi-2\phi-2\phi\cdot\sin^2\eta\cdot\cos^2\phi+\sin^2\eta\cdot\cos\phi\cdot\sin\phi\\
&+\phi\cdot\sin^2\eta+2\cdot\cos^2\eta\cdot\cos\phi\cdot\sin\phi+2\phi\cdot\cos^2\eta+2\phi_2\cdot\sin^2\eta\cdot\cos^2\phi)\\
&+\frac{D^2\sin\eta}{16E\cdot J\cdot\cos^2\eta}(2\phi_2\cdot\sin^2\eta\cdot\cos^2\phi-2\phi\cdot\sin^2\eta\cdot\cos\phi+\sin^2\eta\cdot\cos\phi\cdot\sin\phi\\
&+\phi\cdot\sin^2\eta+2\cos^2\eta\cdot\cos\phi\cdot\sin\phi+2\phi\cdot\cos^2\eta)\\
&+D^2\cdot\sin\eta(2\phi_2\cdot\cos^2\phi-\cos\phi\cdot\sin\phi-\phi-2\phi\cdot\cos^2\phi)\left(\frac{1}{16GK}+\frac{1}{16E\cdot I\cdot\cos^2\eta}\right)
\end{aligned}
$$

$$
\begin{aligned}
h_{32}=&\frac{D\cdot\cos\eta}{8E\cdot A}(2\phi_2\cdot\sin^4\eta\cdot\cos\phi\cdot\sin\phi-2\cos^2\phi-2\cos^4\eta\cdot\cos^2\phi\\
&+2\phi_2^2\cdot\sin^4\eta\cdot\cos^2\phi+4\cos^2\eta\cdot\cos^2\phi-4\phi\cdot\phi_2\cdot\sin^4\eta\cdot\cos^2\phi\\
&-2\phi\cdot\sin^4\eta\cdot\cos\phi\cdot\sin\phi-\phi^2\cdot\sin^4\eta-4\phi\cdot\cos^2\eta\cdot\sin^2\eta\cdot\cos\phi\cdot\sin\phi\\
&+2\phi\cdot\phi_2\cdot\sin^4\eta+2\phi^2\cdot\sin^4\eta\cdot\cos^2\phi+4\phi\cdot\sin^2\eta\cdot\cos\phi\cdot\sin\phi
\end{aligned}
$$

$$
\begin{aligned}
&+ 4\phi_2 \cdot \cos^2\eta \cdot \sin^2\eta \cdot \cos\phi \cdot \sin\phi - 4\phi_2 \cdot \sin^2\eta \cdot \cos\phi \cdot \sin\phi + \sin^4\eta \cdot \sin^2\phi \\
&+ 2\sin^2\eta \cdot \cos^2\eta \cdot \sin^2\phi - 2 \cdot \sin^2\eta \cdot \sin^2\phi) \\
&+ \frac{D^3}{32E \cdot J \cdot \cos^3\eta}(2\phi^2 \cdot \sin^4\eta \cdot \cos^2\phi - 2\phi \cdot \sin^4\eta \cdot \cos\phi \cdot \sin\phi - \phi^2 \cdot \sin^4\eta \\
&+ \sin^4\eta \cdot \sin^2\phi + 4\phi_2 \cdot \cos^2\eta \cdot \sin^2\eta \cdot \cos\phi \cdot \sin\phi - 2\cos^4\eta \cdot \cos^2\phi \\
&+ 2\phi_2^2 \cdot \sin^4\eta \cdot \cos^2\phi - 4\phi \cdot \phi_2 \cdot \sin^4\eta \cdot \cos^2\phi + 2\phi_2 \cdot \sin^4\eta \cdot \cos\phi \cdot \sin\phi \\
&+ 2\phi \cdot \phi_2 \cdot \sin^4\eta - 4\phi \cdot \cos^2\eta \cdot \sin^2\eta \cdot \cos\phi \cdot \sin\phi + 2\cos^2\eta \cdot \sin^2\eta \cdot \sin^2\phi) \\
&+ \frac{D^3 \sin^2\eta}{32G \cdot K \cdot \cos\eta}(2\phi_2 \cdot \phi - 2\cos^2\phi - 2\phi_2 \cdot \cos\phi \cdot \sin\phi - \phi^2 - \sin^2\phi \\
&+ 2\phi_2^2 \cdot \cos^2\phi + 2\phi \cdot \cos\phi \cdot \sin\phi + 2\phi^2 \cdot \cos^2\phi - 4\phi \cdot \phi_2 \cdot \cos^2\phi) + \frac{D \cdot \cos^2\phi \cdot \cos\eta}{4k \cdot G \cdot A} \\
&- \frac{D^3 \sin^2\eta}{32E \cdot I \cdot \cos^3\eta}(2\phi^2 \cdot \cos^2\phi - 2\phi \cdot \cos\phi \cdot \sin\phi - 4\phi \cdot \phi_2 \cdot \cos^2\phi + 2\phi \cdot \phi_2 \\
&+ 2\phi_2 \cdot \cos\phi \cdot \sin\phi - \phi^2 + \sin^2\phi + 2\phi_2^2 \cdot \cos^2\phi)
\end{aligned}
$$

$$
h_{54} = \frac{2\cos^4\eta \cdot \sin\eta \cdot \cos\phi}{D \cdot E \cdot A} + \frac{D\cos\phi \cdot \sin\eta}{2E \cdot J} - \frac{D\cos\phi \cdot \sin\eta}{2G \cdot K}
$$

$$
\begin{aligned}
h_{55} = &\frac{\sin^2\eta \cdot \cos^3\eta \cdot (\phi - \cos\phi \cdot \sin\phi)}{D \cdot E \cdot A} + \frac{D(\phi - \cos\phi \cdot \sin\phi) \cdot \sin^2\eta}{4E \cdot J \cdot \cos\eta} \\
&+ \frac{D(\phi - \cos\phi \cdot \sin\phi) \cdot \cos\eta}{4G \cdot K} + \frac{D(\phi + \cos\phi \cdot \sin\phi)}{4E \cdot I \cdot \cos\eta}
\end{aligned}
$$

$$
h_{56} = -\frac{\sin^2\eta \cdot \cos^3\eta \cdot \cos^2\phi}{D \cdot E \cdot A} - \frac{D \cdot \cos^2\phi \cdot \sin^2\eta}{4E \cdot J \cdot \cos\eta} - \frac{D \cdot \cos^2\phi \cdot \cos\eta}{4G \cdot K} + \frac{D\cos^2\phi}{4E \cdot I \cdot \cos\eta}
$$

$$
h_{61} = -\frac{\sin^4\eta \cdot \cos\eta \cdot \sin\phi}{E \cdot A} + \frac{D^2 \cdot \sin^2\eta \cdot \sin\phi}{4 \cdot E \cdot J \cdot \cos\eta} + \frac{D^2 \cdot \cos\eta \cdot \sin\phi}{4 \cdot G \cdot K}
$$

$$
\begin{aligned}
h_{62} = &\frac{\cos^2\eta \cdot \sin\eta}{4EA}(-2\phi \cdot \sin^2\eta \cdot \cos\phi \cdot \sin\phi - \phi^2 \cdot \sin^2\eta + \sin^2\eta \cdot \sin^2\phi \\
&+ 2\phi_2 \cdot \sin^2\eta \cdot \cos\phi \cdot \sin\phi + 2\phi \cdot \phi_2 \cdot \sin^2\eta + 2\cos^2\phi - 2\cos^2\eta \cdot \cos^2\phi) \\
&+ \frac{D^2 \sin\eta}{16E \cdot J \cdot \cos^2\eta}(-2\phi \cdot \sin^2\eta \cdot \cos\phi \cdot \sin\phi - \phi^2 \cdot \sin^2\eta + \sin^2\phi \cdot \sin^2\eta \\
&+ 2\phi_2 \cdot \sin^2\eta \cdot \cos\phi \cdot \sin\phi + 2\phi \cdot \phi_2 \cdot \sin^2\eta - 2\cos^2\phi \cdot \cos^2\eta) \\
&+ \frac{D^2 \sin\eta(2\cos^2\phi + 2\phi_2 \cdot \cos\phi \cdot \sin\phi + 2\phi \cdot \phi_2 + \sin^2\phi - 2\phi\cos\phi \cdot \sin\phi - \phi^2)}{16G \cdot K} \\
&+ \frac{D^2 \sin\eta(2\phi \cdot \phi_2 - 2\phi_2 \cdot \cos\phi \cdot \sin\phi + 2\phi \cdot \cos\phi \cdot \sin\phi - \phi^2 - \sin^2\phi)}{16E \cdot I \cdot \cos^2\eta}
\end{aligned}
$$

$$h_{44} = \frac{2\phi \cdot \cos^5 \eta}{D \cdot E \cdot A} + \frac{D \cdot \phi \cdot \cos \eta}{2E \cdot J} + \frac{D \cdot \phi \cdot \sin^2 \eta}{2 \cdot G \cdot K \cdot \cos \eta}$$

$$h_{45} = \frac{2\cos^4 \eta \cdot \sin \eta \cdot \cos \phi}{D \cdot E \cdot A} + \frac{D \cos \phi \cdot \sin \eta}{2E \cdot J} - \frac{D \cos \phi \cdot \sin \eta}{2G \cdot K}$$

$$h_{46} = -\frac{2\cos^4 \eta \cdot \sin \eta \cdot \sin \phi}{D \cdot E \cdot A} - \frac{D \sin \phi \cdot \sin \eta}{2E \cdot J} + \frac{D \sin \phi \cdot \sin \eta}{2G \cdot K}$$

$$\begin{aligned}
h_{33} = {} & \frac{D \cdot \cos \eta}{24EA}(12\phi_2 \cdot \cos^2 \eta \cdot \sin^2 \eta \cdot \cos^2 \phi - 12\phi_2 \cdot \sin^2 \eta \cdot \cos^2 \phi + 6\phi \cdot \phi_2 \cdot \sin^4 \eta \\
& - 6\phi_2^2 \cdot \sin^4 \eta \cdot \cos \phi \cdot \sin \phi + 6\cos^4 \eta \cdot \cos \phi \cdot \sin \phi + 6\phi \cdot \cos^4 \eta \\
& + 3\sin^4 \eta \cdot \cos \phi \cdot \sin \phi + 2\phi^3 \cdot \sin^4 \eta + 3\phi \cdot \sin^4 \phi - 12\cos^2 \eta \cdot \cos \phi \cdot \sin \phi \\
& - 12\phi \cdot \cos^2 \eta - 6\phi \sin^4 \eta \cdot \cos^2 \phi - 6\phi \cdot \sin^2 \eta - 12\phi \cdot \cos^2 \eta \cdot \sin^2 \eta \cdot \cos^2 \phi \\
& + 6\phi \cdot \cos^2 \eta \cdot \sin^2 \eta - 6\sin^2 \eta \cdot \cos \phi \cdot \sin \phi + 12\phi \cdot \sin^2 \eta \cdot \cos^2 \phi \\
& + 6\cos^2 \eta \cdot \sin^2 \eta \cdot \cos \phi \cdot \sin \phi - 6\phi^2 \cdot \sin^4 \eta \cdot \cos \phi \cdot \sin \phi + 12\phi \cdot \phi_2 \cdot \sin^4 \eta \cdot \cos \phi \cdot \sin \phi \\
& - 6\phi^2 \cdot \phi_2 \cdot \sin^4 \eta - 6\phi_2 \cdot \sin^4 \eta \cdot \sin^2 \phi + 6\cos \phi \cdot \sin \phi + 6\phi) \\
& + \frac{D^3}{96E \cdot J \cdot \cos^3 \eta}(3\phi \cdot \sin^4 \eta + 6\cos^4 \eta \cdot \cos \phi \cdot \sin \phi + 6\phi \cdot \cos^4 \eta - 6\phi^2 \cdot \phi_2 \cdot \sin^4 \eta \\
& - 6\phi_2 \cdot \sin^4 \eta \cdot \sin^2 \phi + 12\phi_2 \cdot \cos^2 \eta \cdot \sin^2 \eta \cdot \cos^2 \phi - 6\phi^2 \cdot \sin^4 \eta \cdot \cos \phi \cdot \sin \phi \\
& + 2\phi^3 \cdot \sin^4 \eta - 6\phi \cdot \sin^4 \eta \cdot \cos^2 \phi + 3\sin^4 \eta \cdot \cos \phi \cdot \sin \phi + 6\phi \cdot \phi_2^2 \cdot \sin^4 \eta \\
& + 12\phi \cdot \phi_2 \cdot \sin^4 \eta \cdot \cos \phi \cdot \sin \phi - 6\phi_2^2 \cdot \sin^4 \eta \cdot \cos \phi \cdot \sin \phi - 12\phi \cdot \cos^2 \eta \cdot \sin^2 \eta \cdot \cos^2 \phi \\
& + 6\cos^2 \eta \cdot \sin^2 \eta \cdot \cos \phi \cdot \sin \phi + 6\phi \cdot \cos^2 \eta \cdot \sin^2 \eta) \\
& + \frac{D^3 \sin^2 \eta}{96G \cdot K \cdot \cos \eta}(6\phi \cdot \cos^2 \phi - 6\phi_2^2 \cos \phi \cdot \sin \phi - 6\phi^2 \cdot \cos \phi \cdot \sin \phi + 2\phi^3 + 3\phi \\
& + 12\phi \cdot \phi_2 \cdot \cos \phi \cdot \sin \phi - 6\phi^2 \cdot \phi_2 - 6\phi_2 \cdot \sin^2 \phi + 6\phi \cdot \phi_2^2 - 12\phi_2 \cdot \cos^2 \phi + 3\cos \phi \cdot \sin \phi) \\
& + \frac{D(\phi - \cos \phi \cdot \sin \phi + \sin^2 \eta \cdot \cos \phi \cdot \sin \phi + \phi \cdot \sin^2 \eta)}{4k \cdot G \cdot A \cdot \cos \eta} \\
& + \frac{D^3 \sin^2 \eta}{96E \cdot I \cdot \cos^3 \eta}(6\phi \cdot \cos^2 \phi + 6\phi_2^2 \cos \phi \cdot \sin \phi + 6\phi^2 \cos \phi \cdot \sin \phi + 2\phi^3 \\
& - 12\phi \cdot \phi_2 \cos \phi \cdot \sin \phi - 6\phi^2 \cdot \phi_2 + 6 \cdot \phi_2 \cdot \sin^2 \phi + 6\phi \cdot \phi_2^2 - 3\cos \phi \cdot \sin \phi - 3\phi)
\end{aligned}$$

$$\begin{aligned}
h_{34} = {} & -\frac{\cos^3 \eta \cdot (\cos^2 \eta \cdot \sin \phi + \phi_2 \cdot \sin^2 \eta \cdot \cos \phi + \sin^2 \eta \cdot \sin \phi - \phi \cdot \sin^2 \eta \cdot \cos \phi - \sin \phi)}{EA} \\
& - \frac{D^2(\cos^2 \eta \cdot \sin \phi + \phi_2 \cdot \sin^2 \eta \cdot \cos \phi - \phi \cdot \sin^2 \eta \cdot \cos \phi + \sin^2 \eta \cdot \sin \phi)}{4E \cdot J \cdot \cos \eta} \\
& + \frac{D^2(\phi_2 - \phi) \cdot \sin^2 \eta \cdot \cos \phi}{4G \cdot K \cos \eta}
\end{aligned}$$

$$h_{35} = -\frac{\cos^2\eta\cdot\sin\eta}{4EA}(2\phi\cdot\sin^2\eta\cdot\cos\phi\cdot\sin\phi-\phi^2\cdot\sin^2\eta-\sin^2\eta\cdot\sin^2\phi-2\cos^2\phi$$
$$+2\cos^2\eta\cdot\cos^2\phi-2\phi_2\cdot\sin^2\eta\cdot\cos\phi\cdot\sin\phi+2\phi\cdot\phi_2\cdot\sin^2\eta)$$
$$-\frac{D^2\sin\eta}{16E\cdot J\cdot\cos^2\eta}(2\phi\cdot\sin^2\eta\cdot\cos\phi\cdot\sin\phi-\phi^2\cdot\sin^2\eta-\sin^2\eta\cdot\sin^2\phi$$
$$-2\phi_2\cdot\sin^2\eta\cdot\cos\phi\cdot\sin\phi+2\phi\cdot\phi_2\cdot\sin^2\eta+2\cos^2\eta\cdot\cos^2\phi)$$
$$-\frac{D^2\cdot\sin\eta(-2\cos^2\phi-2\phi_2\cdot\cos\phi\cdot\sin\phi+2\phi\cdot\phi_2+2\phi\cdot\cos\phi\cdot\sin\phi-\phi^2-\sin^2\phi)}{16GK}$$
$$-\frac{D^2\sin\eta(2\phi_2\cdot\cos\phi\cdot\sin\phi+2\phi\cdot\phi_2-2\phi\cdot\cos\phi\cdot\sin\phi-\phi^2+\sin^2\phi)}{16E\cdot I\cdot\cos^2\eta}$$

$$h_{36} = \frac{\cos^2\eta\cdot\sin\eta}{4EA}(-2\cos\phi\cdot\sin\phi-2\phi-2\phi\cdot\sin^2\eta\cdot\cos^2\phi+\sin^2\eta\cdot\cos\phi\cdot\sin\phi$$
$$+\phi\cdot\sin^2\eta+2\cdot\cos^2\eta\cdot\cos\phi\cdot\sin\phi+2\phi\cdot\cos^2\eta+2\phi_2\cdot\sin^2\eta\cdot\cos^2\phi)$$
$$+\frac{D^2\sin\eta}{16E\cdot J\cdot\cos^2\eta}(2\phi_2\cdot\sin^2\eta\cdot\cos^2\phi-2\phi\cdot\sin^2\eta\cdot\cos\phi+\sin^2\eta\cdot\cos\phi\cdot\sin\phi$$
$$+\phi\cdot\sin^2\eta+2\cos^2\eta\cdot\cos\phi\cdot\sin\phi+2\phi\cdot\cos^2\eta)$$
$$+D^2\cdot\sin\eta(2\phi_2\cdot\cos^2\phi-\cos\phi\cdot\sin\phi-\phi-2\phi\cdot\cos^2\phi)\left(\frac{1}{16GK}+\frac{1}{16E\cdot I\cdot\cos^2\eta}\right)$$

$$h_{41} = \frac{\phi\cdot\cos^2\eta\cdot\sin^3\eta}{E\cdot A}-\frac{D^2\cdot\phi\cdot\sin\eta}{4\cdot E\cdot J}+\frac{D^2\cdot\phi\cdot\sin\eta}{4\cdot G\cdot K}$$

$$h_{42} = -\frac{\cos^3\eta(\cos\phi-\cos^2\eta\cdot\cos\phi-\phi\cdot\sin^2\eta\cdot\sin\phi-\sin^2\eta\cdot\cos\phi+\phi_2\cdot\sin^2\eta\cdot\sin\phi)}{EA}$$
$$-\frac{D^2(\phi_2\cdot\sin^2\eta\cdot\sin\phi-\cos^2\eta\cdot\cos\phi-\phi\cdot\sin^2\eta\cdot\sin\phi-\sin^2\eta\cdot\cos\phi)}{4E\cdot J\cdot\cos\eta}$$
$$+\frac{D^2(\phi_2-\phi)\sin^2\eta\cdot\sin\phi}{4G\cdot K\cdot\cos\eta}$$

$$h_{43} = -\frac{\cos^3\eta\cdot(\cos^2\eta\cdot\sin\phi+\phi_2\cdot\sin^2\eta\cdot\cos\phi+\sin^2\eta\cdot\sin\phi-\phi\cdot\sin^2\eta\cdot\cos\phi-\sin\phi)}{EA}$$
$$-\frac{D^2(\cos^2\eta\cdot\sin\phi+\phi_2\cdot\sin^2\eta\cdot\cos\phi-\phi\cdot\sin^2\eta\cdot\cos\phi+\sin^2\eta\cdot\sin\phi)}{4E\cdot J\cdot\cos\eta}$$
$$+\frac{D^2(\phi_2-\phi)\cdot\sin^2\eta\cdot\cos\phi}{4G\cdot K\cos\eta}$$

$$h_{51} = \frac{\sin^4\eta\cdot\cos\eta\cdot\cos\phi}{E\cdot A}-\frac{D^2\cdot\sin^2\eta\cdot\cos\phi}{4\cdot E\cdot J\cdot\cos\eta}-\frac{D^2\cdot\cos\eta\cdot\cos\phi}{4\cdot G\cdot K}$$

$$
\begin{aligned}
h_{52} = & -\frac{\cos^2\eta\cdot\sin\eta}{4EA}(2\phi_2\cdot\sin^2\eta\cdot\cos^2\phi+2\cos^2\eta\cdot\cos\phi\cdot\sin\phi-2\phi\cdot\cos^2\eta \\
& -2\phi\cdot\sin^2\eta\cdot\cos^2\phi+\sin^2\eta\cdot\cos\phi\cdot\sin\phi+\phi\cdot\sin^2\eta-2\cos\phi\cdot\sin\phi+2\phi) \\
& -\frac{D^2\sin\eta}{16E\cdot J\cdot\cos^2\eta}(\sin^2\eta\cdot\cos\phi\cdot\sin\phi-2\phi\cdot\sin^2\eta\cdot\cos^2\phi+\phi\cdot\sin^2\eta \\
& +2\phi_2\cdot\sin^2\eta\cdot\cos^2\phi+2\cos^2\eta\cdot\cos\phi\cdot\sin\phi-2\phi\cdot\cos^2\eta) \\
& -\frac{D^2\sin\eta(-2\phi\cdot\cos^2\phi-\cos\phi\cdot\sin\phi+3\phi+2\phi_2\cdot\cos^2\phi)}{16G\cdot K} \\
& +\frac{D^2\sin\eta(\phi-2\phi\cdot\cos^2\phi+\cos\phi\cdot\sin\phi+2\phi_2\cdot\cos^2\phi)}{16E\cdot I\cdot\cos^2\eta}
\end{aligned}
$$

$$
\begin{aligned}
h_{53} = & -\frac{\cos^2\eta\cdot\sin\eta}{4EA}(2\phi\cdot\sin^2\eta\cdot\cos\phi\cdot\sin\phi-\phi^2\cdot\sin^2\eta-\sin^2\eta\cdot\sin^2\phi-2\cos^2\phi \\
& +2\cos^2\eta\cdot\cos^2\phi-2\phi_2\cdot\sin^2\eta\cdot\cos\phi\cdot\sin\phi+2\phi\cdot\phi_2\cdot\sin^2\eta) \\
& -\frac{D^2\sin\eta}{16E\cdot J\cdot\cos^2\eta}(2\phi\cdot\sin^2\eta\cdot\cos\phi\cdot\sin\phi-\phi^2\cdot\sin^2\eta-\sin^2\eta\cdot\sin^2\phi \\
& -2\phi_2\cdot\sin^2\eta\cdot\cos\phi\cdot\sin\phi+2\phi\cdot\phi_2\cdot\sin^2\eta+2\cos^2\eta\cdot\cos^2\phi) \\
& -\frac{D^2\cdot\sin\eta(-2\cos^2\phi-2\phi_2\cdot\cos\phi\cdot\sin\phi+2\phi\cdot\phi_2+2\phi\cdot\cos\phi\cdot\sin\phi-\phi^2-\sin^2\phi)}{16GK} \\
& -\frac{D^2\sin\eta(2\phi_2\cdot\cos\phi\cdot\sin\phi+2\phi\cdot\phi_2-2\phi\cdot\cos\phi\cdot\sin\phi-\phi^2+\sin^2\phi)}{16E\cdot I\cdot\cos^2\eta}
\end{aligned}
$$

References

[1] P.J. Agnew, Functional effectiveness of a myoelectric prosthesis compared with a functional split hook prosthesis: a single subject experiment, Prost. Orth. Int. 5 (1981) 92–96.

[2] S.E. Baek, S.H. Lee, J.H. Chang, Design and control of a robotic finger for prosthesis hands, in: Proc. Int. Conf. Intelligent Robots and Systems, 1999, pp. 113–117.

[3] J.C. Cool, J. Kruit, Myopneumatic hand prosthesis for children, J. Med. Eng. Technol. 13 (1989) 129–133.

[4] M.E. Cupo, S.J. Sheredos, Clinical evaluation of a new, above elbow, body powered prosthesis arm: a final report, J. Rehabil. Res. Dev. 35 (1998) 338–395.

[5] M.R. Cutkosky, Robotic Grasping and Fine Manipulation, Kluwer Acadmic Publishers, Boston, 1985.

[6] J. Demmel, G. Lafferriere, J. Schwartz, M. Sharir, Theoretical and experimental studies using a multifinger planar manipulator, in: IEEE International Conference on Robotics and Automation, 1988, pp. 390–395.

[7] R. Doshi, C. Yeh, M. LeBlanc, The design and development of a gloveless endoskeletal prosthetic hand, J. Rehabil. Res. Develop. 35 (4) (1998) 388–395.

[8] G. Figliolini, M. Ceccarelli, A motion analysis for one d.o.f. anthropomorphic finger mechanism, in: Proceedings of DETC^{TM} 98, Atlanta, 1998.

[9] M.J. Fletcher, New developments in hands and hooks, in: P.E. Klopsteg, P.D. Wilson (Eds.), Human Limbs and Their Substitutes, Hafner Publishing Company, New York, 1968, pp. 222–238 (Reprint of 1954).

[10] A.K. Godden, Some factors in the design of an adaptive artificial hand, in: Symposium on the Basic Problems of Prehension, Movement and Control of Artificial Limbs, The Institution of Mechanical Engineers, London, 30th October and 1st November 1968.
[11] G. Guo, X. Qian, W.A. Gruver, Single degree of freedom multi-function prosthetic hand mechanism with an automatically variable speed transmission, in: 22nd Biennial Mechanisms Conference ASME 1992, Robotics, Spatial Mechanisms and Mechanical Systems, ASME Design Engineering Division DE v 45, 1992, pp. 149/154.
[12] H. Hanafusa, H. Asada, A robotic hand with elastic fingers and its application to assembly process, MIT Press, 1982, pp. 337–360.
[13] J.L. Herder, J.C. Cool, D.H. Plettenburg, Voluntary pinching, in: Conference Book IXth World Congress ISPO, Amsterdam, The Netherlands, ISPO Publications, Copenhagen, Denmark, 1998, pp. 466–468.
[14] J.L. Herder, J.C. Cool, D.H. Plettenburg, Methods for reducing energy dissipation in cosmetic gloves, J. Rehabil. Res. Dev. 35 (2) (1998) 201–209.
[15] S. Jacobsen, J. Wood, K. Bigger, E. Iverson, The utah/mit hand: work in progress, Int. J. Robot. Res. 4 (3) (1984) 21–50.
[17] P.E. Klopsteg, P.D. Wilson, Human Limbs and Their Substitutes, Hafner Publishing Company, New York, 1968 (Reprint of 1954).
[18] J. Kruit, J.C. Cool, Body powered hand prosthesis with low operating power for children, J. Med. Eng. Technol. 13 (1/2) (1989) 129–133.
[19] J.P. Kuntz, Rolling Link Mechanisms, PhD thesis, Delft University of Technology, 1995.
[20] P.J. Kyberd, P.H. Chappell, The southampton hand, an intelligent myoelectric prosthesis, J. Rehabil. Res. Develop. 31 (4) (1994) 326–334.
[21] P.J. Kyberd, M. Evans, S. te Winkel, An intelligent anthropomorphic hand, with automatic grasp, Robotica 16 (1998) 531–536.
[22] T. Laliberté, C.M. Gosselin, Simulation and design of underactuated mechanical hands, Mech. Mach. Theory 33 (1/2) (1998) 39–57.
[23] L. Lindkvist, Three-dimensional Load–Deformation Relationships of Arbitrarily Loaded Coiled Springs, Chalmers University of Technology, Goteborg, Sweden, 1995.
[24] N.G.A. van Leerdam, The Swinging UTX Orthosis, Biomechanical Fundamentals and Conceptual Design, PhD thesis, University of Twente, Enschede, The Netherlands, 1993.
[25] A. van Lunteren, G.H.M. van Lunteren-Gerritsen, H.G. Stassen, M.J. Zuithoff, A field evaluation of arm prostheses for unilateral amputees, Prost. Orth. Int. 7 (1983) 141–151.
[26] M.T. Mason, J.K. Salisbury, Robot Hands and the Mechanics of Manipulation, MIT Press, 1985.
[27] E.F. Murphy, Manipulators and upper-extremity prosthetics, Bulletin of Prosthetics Research, Fall: 107–117. NASA, 1985, Low friction joint for robot fingers, l NASA Tech Briefs, 1964, p. 140.
[28] R.M. Murray, S.S. Sastry, Control experiments in planar manipulation and grasping, in: IEEE International Conference on Robotics and Automation, 1990, pp. 624–629.
[29] V.-D. Nguyen, Constructing force-closure grasps, Int. J. Robot. Res. 7 (3) (1988) 3–16.
[30] T. Okada, Computer control of multijointed finger system for precise object-handling, IEEE Trans. Syst. Man Cybernet. SMS-12 (3) (1982) 289–299.
[32] D.H. Plettenburg, J.C. Cool, Upper extremity prostheses, the WILMER approach, in: Proceedings 7th World Congress of ISPO, Chicago, 1992.
[33] D.H. Plettenburg, Myopneumatic hand prosthesis for children, J. Rehabil. Sci. 1 (1988) 135–137.
[34] B. Radocy, Voluntary closing control: a successful new design approach to an old concept, Clin. Prost. Orth. 10 (2) (1986) 82–86.
[35] D.H. Silcox, M.D. Rooks, R.R. Vogel, L.L. Fleming, Myoeletric prosthesis, J. Bone Joint Surg. 75 (1993) 1781–1789.
[36] F. Skinner, Designing a multiple prehension manipulator, J. Mech. Eng. 97 (9) (1975) 30–37.
[37] R. Vinet, Y. Lozach, N. Beadry, G. Drouin, Design methodology for a multifunctional hand prosthesis, J. Rehabil. Res. Develop. 32 (4) (1995) 316–324.
[38] J. Yang, P. Esteban, K. Abdel-Malek, Design and analysis of an inherently-compliant light-weight active hand prosthesis, in: Proceedings of 2002 ASME Design Engineering Technical Conferences, Montreal, Canada, DETC2002/MECH-34297, September 29–October 2, 2002.